

TASK 3.1.3

S-PARAMETER BASED FRAMEWORK FOR ANALYSIS OF COMMON MODE COUPLINGS BETWEEN MVDC POWER APPARATUS

Year One – Deliverable(s)

Submitted to:
The Office of Naval Research

Contract: N00014-14-1-0198

Submitted by:
FSU - L. Graber (Lead), M. Steurer

MSU – M. Mazzola, A. Card

01/14/2015



1 TASK DESCRIPTION

S-parameters are needed when one is attempting to characterize/measure the wide-bandwidth behavior of power systems, including switching-induced electromagnetic fields, and the behavior of the system in response to faults. This promising approach has been investigated on a very limited set of components. This task will expand the work into the realm of MW scale equipment by analyzing such devices already existing in ESRDC labs. Power electronics converters of the megawatt class need to be characterized regarding their capacitive, inductive, resistive and radiative coupling to the ground plane. This will be accomplished by S-parameter measurement using a vector network analyzer (VNA). The main converters of interest are the 5-MW variable voltage source inverter at CAPS, the MVDC converters to be installed at CAPS before the end of 2013, various medium scale converters also available at CAPS, and the converters of the 750-V testbed at Purdue University. These converters are ungrounded by design. However, they do have a parasitic impedance to ground that can be measured by VNA measurements while not energized and by fault tests when in operation. Additional impedances to ground can be added for calibration purposes.

2 YEAR ONE DELIVERABLES

- Initial guidelines on determination of ground impedances on cables, rotating machines, and large power electronic converters
- Database updates for common mode coupling attributes in the Power Interconnection Calculator (coordinated with Task 2.8.1 conducted by MSU)

3 APPENDIX OF REPORTS SUBMITTED

- A. Technical Report: S-Parameter Based Framework for Analysis of Common Mode Couplings Between MVDC Power Apparatus
- B. Paper – Validation of a Scattering Parameter Based Model of a Power Cable for Shipboard Grounding Studies
- C. Paper – Implementing S-parameter Models in MATLAB Simulink to Analyze Transients in Ungrounded Shipboard Power Systems
- D. Paper – Challenges of frequency domain measurement for modeling the components of shipboard power systems
- E. Paper – High Frequency Models for Rotating Machines in Ungrounded Shipboard Power Systems
- F. Presentation – Modeling of Common-mode Currents on Electric Ship Architectures

APPENDIX A

S-PARAMETER BASED FRAMEWORK FOR ANALYSIS OF COMMON MODE COUPLINGS BETWEEN MVDC POWER APPARATUS (TASK 3.1.3)

Technical Report

Submitted to:
The Office of Naval Research

Contract Number: N0014-08-1-0080

Submitted by:
L. Graber, M. Steurer, M. Mazzola, A. Card

January 2015

Approved for Public Release – Distribution Unlimited

Any opinions, findings, conclusions or recommendations expressed in this publication are those of the author(s) and do not necessarily reflect the views of the Office of Naval Research.

1 EXECUTIVE SUMMARY

The ESRDC Task 3.1.3 Group has been working on developing new approaches for modeling the common mode characteristics of the power systems components, which are expected to be seen onboard a MW scale all-electric ship. In 2013, the characterization started by using S-parameters to model the power cables as the best understood part of the system, which has potentially the greatest contribution to the parasitic coupling between the power system and the ship hull ground. This has been documented in the article “Implementing S-parameter Models in MATLAB Simulink to Analyze Transients in Ungrounded Shipboard Power Systems” [2]. Also in 2013, the ability of the cable models to predict the fault responses was tested by means of a fast MOSFET circuit that can resemble a short circuit when activated. The details of the modeling process and the experiment setup are explained in the first paper titled “Validation of a Scattering Parameter Based Model of a Power Cable for Shipboard Grounding Studies” [1].

Once it was determined that the S-parameter based models can be useful for fault studies we proceeded to apply the method on other components such as rotating machines and power converters. Since scattering parameters measurement is not common for power system devices, there was a need for a systematic approach to determine how to perform highly accurate frequency domain measurements on large machines. The Vector Network Analyzer (Scattering parameter measurement instrument) and the device under test (DUT) cannot be connected directly due to the difference between the size of the terminals of the power devices and the terminals of the VNA. The connectors designed for this purpose impose a limitation on the frequency bandwidth in which the measurement is valid. The challenges with respect to the measurement and our approach to address them are explained in the paper titled “Challenges of Frequency Domain Measurement for Modeling the Components of the Shipboard Power System” [3]. The important VNA settings such as higher and lower frequency limits and the intermediate frequency bandwidth are also documented. Finally, the results of the scattering parameter measurement of a helium gas cooled superconducting cable are presented as an example.

The aforementioned method was used to measure the scattering parameters of a permanent magnet synchronous machine (PMSM). The models based on lumped components cannot accurately predict the fault responses. This was demonstrated by comparing the results of a lumped-element based model of the machine after faulting one phase to ground with the experimental results of the same scenario when the machine was operating at nominal speed. The model results presented in the paper titled “High Frequency Models for Rotating Machines in Ungrounded Shipboard Power Systems” [4] show that the predicted current peak is approximately two times greater than the measured value in the experiment. New models based on distributed components are currently under consideration.

The next step for the ESRDC Task 3.1.3 Group is to investigate parasitic coupling effects of the power converters and motor drives and study the essential factors or parts of the devices that affect the overall parasitic coupling to ground. These factors can be the position of bus bars relative to the grounded enclosure, the output (line) filters, the capacitance between the power semiconductors, heat sinks, and the power electronics enclosure, and potentially present isolation transformers. Determining the influence of each of these factors can help in deciding which part can be neglected with respect to coupling to ground as well as determining how to take the parasitic coupling into account in currently existing models.

To complete the capability for ship designers to understand common-mode current flow and its mitigation, a modeling and simulation process is required that “completes the circuit.” Therefore, a computationally practical method for modeling common-mode current on the ship hull and structures bonded to it, including equipment chassis’ and cable armored sheaths, is needed. Fortunately, the S-parameter behavioral modeling approach described above for internal coupling in major power components is also a good choice for open-form conductor modeling, such as the ship hull.

A method of discretizing a CAD rendering of a ship hull structure into an S-parameter model of the open-form conductor system it represents was presented in [5] to satisfy the need for a tool that is computationally much easier to implement than existing finite-element methods. The approach taken is to discretize with component behavioral models, each derived from physics-based modeling, as opposed to discretization of the entire structure with difference equations and a spatial mesh. In this approach, discrete elementary ship hull “sections” are defined in the CAD entry tool in a physics-based modeling software suite called ADS (supported by Agilent Technologies, Inc.). This elementary section is typically 1 m^2 and includes various layers to model ship steel (including magnetic properties), dielectric interfaces such as paint and air, and a semi-infinite conducting body representing seawater. Each elementary section has a centrally located port and edge-located ports around the perimeter. ADS extracts the S-parameter model between the central port and all edge ports. Then, a system of elementary S-parameter models are wire-bonded together to form an approximation to the shape of the ship hull or key internal structures, such as major bulkheads. In a second S-parameter extraction step the edge ports “disappear” into an equivalent behavioral model of the complete surface, leaving the central ports externally visible to the final engineering user of the complete behavioral model. The model of the complete surface is left with electrical “grounding” contact points, which are the ports of the S-parameter model formed by each central point in the original elementary sections. These represent possible bonding points for the equipment models described above, such as grounded machine chassis’ and cable sheaths. This allows a finite but otherwise flexibly large number of permutations to be used to quickly build a valid common-mode behavioral model of the hull/bulkhead conduction paths. The behavioral model of the hull/bulkhead can be combined with other S-parameter models of equipment and lumped circuit elements like inductances and sources and then solved for voltages and currents (versus time or frequency) with standard circuits-aware software tools such as SimPowerSystems in Matlab/Simulink.

The computational simplification arises by reducing the number of simultaneously solved algebraic equations to approximately the number of bonding points, rather than the much larger number of equations defined by a geometrically massive finite-element mesh of the whole structure. The only material loss in fidelity need be the finite access to solution points on the surface, which is limited to the central ports of each original elementary section. However, this discretization of access points is similar to what happens on board real ships, where “access points” in the model are equivalent to localized bonding points in the grounding system. The underlying fidelity of the model is equivalent or superior to the alternatives because the elementary sections are themselves based on well-meshed finite-element physical models solved during the first S-parameter extraction step. This method has been validated by comparison to known electromagnetic solutions.

2 PUBLISHED WORK IN YEAR 2014

The research performed under ESRDC Task 3.1.3 has been documented in form of peer-reviewed publications. Hence, the publications are integral part of this end of year report.

- [1] Mohebali, B.; Breslend, P.; Graber, L.; & Steurer, M., “Validation of a Scattering Parameter Based Model of a Power Cable for Shipboard Grounding Studies,” ASNE Electric Machines Technology Symposium, Philadelphia, PA, 28-29 May 2014.
- [2] Kofler, M.; Benson, R.A.; & Graber, L., “Implementing S-parameter Models in MATLAB Simulink to Analyze Transients in Ungrounded Shipboard Power Systems,” Naval Engineers Journal, December 2014.
- [3] Mohebali, B.; Breslend, P.; Graber, L.; & Steurer, M., “Challenges of frequency domain measurement for modeling the components of shipboard power systems,” accepted for publication in the Naval Engineers Journal.
- [4] Breslend, P.; Mohebali, B.; Graber, L.; & Steurer, M., “High Frequency Models for Rotating Machines in Ungrounded Shipboard Power Systems,” accepted for publication in the Naval Engineers Journal.
- [5] Mazzola, M; & Rahmani, M., “Modeling of Common-mode Currents on Electric Ship Architectures,” Southeastern Symp. Contemporary Engineering Topics, New Orleans, LA, 19 Sept. 2014.

APPENDIX B

Validation of a Scattering Parameter Based Model of a Power Cable for Shipboard Grounding Studies

Behshad Mohebbali, Patrick Breslend, Lukas Graber, Michael Steurer

Abstract—The choice of the grounding strategy for 100 MW scale shipboard power systems envisioned for future all-electric surface warships is of high importance since it will greatly affect the system response to different fault scenarios. Recent research has indicated that conventional modeling approaches, in which the system components were modeled as lumped elements, fail to accurately predict the characteristics of the transient response of shipboard power systems to ground faults. Therefore, a modeling method based on the scattering parameters (s-parameters) of the system components has been developed. This paper introduces an approach for validating s-parameter based models of shipboard components such as power cables, power converters, and rotating machines by comparing experimental results with simulation results in the time domain. Firstly, the simulation model is briefly discussed. Secondly, the validation approach is described. Thirdly, the hardware circuit used for the experiment is explained in detail. Finally, the results from the model and the experiment is compared and analyzed. Having an accurate and reliable simulation model is necessary for choosing the best grounding strategy for power systems of future all-electric ships.

Index Terms—Ungrounded power systems, transients, common-mode currents, simulation model

I. INTRODUCTION

THE grounding strategy for future all-electric ships has a considerable impact on the performance characteristics of the ship including the fault capabilities, voltage transients, electromagnetic compatibility and the electromagnetic signature of the ship. There are three basic grounding strategies: Ungrounded (also known as unintentionally grounded), solidly grounded, and high impedance grounded [1]. Ungrounded power systems offer the benefit of allowing continuation of service during a single rail to ground fault. This comes with an increased level of rail harmonics and a risk for more pronounced transient over voltages during switching and fault events [2]. By carefully choosing high impedance elements to ground and their optimal location in the power system, over voltage effects can be minimized. Simulation models are needed to carefully design the grounding strategy and balance the different effects such as DC rail to ground voltage ripple, maximum over voltage during transients, common mode currents in the ship hull, and power dissipation in the grounding elements [2].

In earlier publications [3]–[5] we introduced scattering parameters as a tool to validate simulation models and their suitability for modeling shipboard power systems. Scattering parameters (S-parameters) are network parameters in the

frequency domain that describe n-port linear time-invariant networks by means of reflection and transmission coefficients at a given frequency vector [6]. They can be obtained by measurement using a vector network analyzer or by simulation models based on circuits or finite elements. S-parameter data can be incorporated in simulation models directly or by extracting a model based on lumped elements. Some simulation software packages support S-parameters natively, while others require the user to setup the necessary framework.

A simplified model of DC power distribution on a ship with special emphasis on coupling to ground is shown in Fig. 1. Each subsystem is represented by a block. The subsystems couple locally to the ship hull. The model of the ship hull allows for individual ground potentials and therefore the simulation of common mode currents. This can be important for studying the impact of a certain grounding scheme to the electromagnetic signature of the ship. It would also allow to model potential interference with the cathodic protection system or the degaussing system.

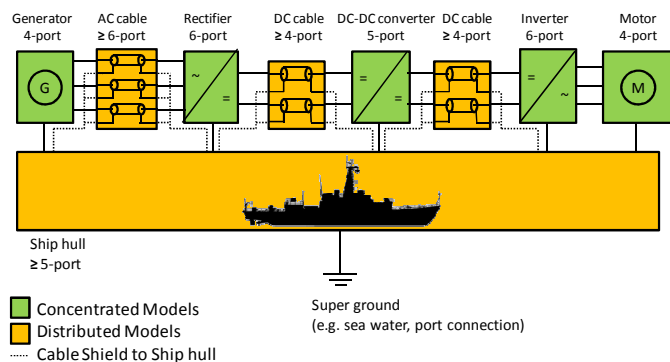


Fig. 1 Simplified model of DC power distribution. Each block represents a linear time-invariant (LTI) network defined by S-parameters. Each block is grounded by a local connection to the ship hull. The ship hull assumes ground potential at a single location only (“super ground”).

Some of the subsystems in Fig. 1 have small physical dimensions and can therefore be assumed to be concentrated models. The term “small” must be seen in relation to the wavelength of the highest frequency of interest. This category typically includes power electronic converters and rotating machines. Other subsystems have large physical dimensions that can have length scales of the same order of magnitude as the wavelength of the fastest transients. Typical examples for distributed models are power cables and the ship hull. Concentrated models can usually be modeled using lumped elements while distributed models sometimes require the use

of more sophisticated models that can be based on scattering parameters or other types of network parameters.

The importance of studying the coupling to ground of ungrounded systems by developing more accurate models is shown by an example of a fault scenario. Fig. 2 shows a bipolar DC source of ± 10 kV powering a $10\ \Omega$ resistive load via a cable. The DC source is essentially ungrounded; however, a $100\ \text{k}\Omega$ resistor from midpoint to ground is added for numerical reasons while keeping the system de-facto ungrounded. The positive and negative rails each consist of two 25 m cable segments in series. They are represented by pie models developed based on the resistance, inductance, and capacitance per length provided by the manufacturer. The system is loaded with a $10\ \Omega$ resistive load. The model is simulated by MATLAB Simulink SimPowerSystems toolbox. At $t = 0$ s, a ground fault occurs at the center point of the negative rail, causing the negative rail to be shorted to ground. The transient voltage response on the source side is shown in Fig. 3. Even though the voltage between the two rails maintains a constant value of 20 kV at all times, the positive rail voltage peak is 28.5 kV. Since the cable shields are connected to the ground and the normal operating voltage of the cables is 10 kV, the cables might not have been designed to tolerate such a large transient voltage and the cable insulation could therefore get damaged. Having accurate models of the system coupling to ground helps the designer engineers to have a better understanding of the scale and the nature of such transients.

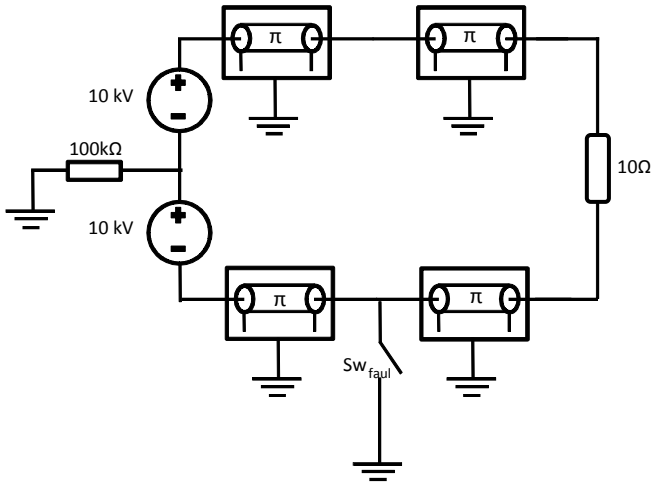


Fig. 2 The schematic of an MVDC system in MW scale. The cables on the system are modeled by single section pie models. The fault occurs at the middle of the negative rail.

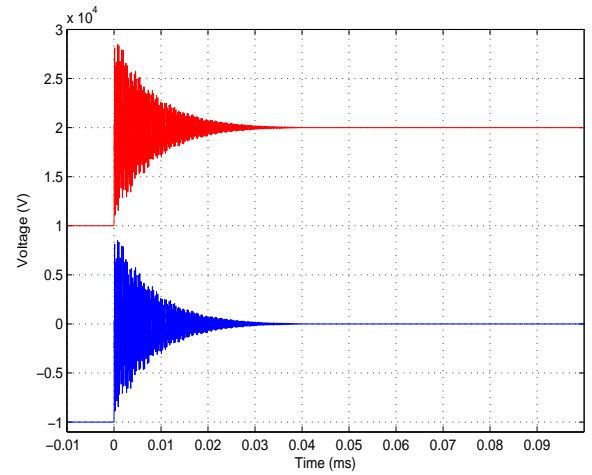


Fig. 3 The simulation results transient response of a shipboard power system to a ground fault in the middle of the negative leg of the DC rail. The red line is the positive rail voltage and the blue line is the negative rail voltage. Even though the voltage difference between the rails remains constant, however, the voltage in positive rail reaches 28.5 kV which can lead to insulation damage.

II. EXTRACTION OF S-PARAMETER MODELS

The first step to obtain S-parameter models consists of measuring or simulating s-parameters of the device under test (DUT). A 2-port vector network analyzer (VNA) has been used to measure the scattering parameters of a 5 kV XLPE single conductor power cable. The choice of using a power cable was due to its passive nature, the variety of available methods for modeling it which can facilitate the validation process and the pronounced coupling to ground [7]. The frequency range in which the measurement has been performed is limited from 10 Hz to 10 MHz. Cable leads from the instrument to the power component are of special interest: Since high power components do not feature high frequency (coaxial) connectors, wires have to be attached to bus bars using rudimentary methods. This limits the upper frequency limit since the variable geometry of the wires does not allow for phase-stable measurements above a certain frequency. Tests conducted on a superconducting power cable resulted in an upper frequency limit of around 10 MHz. Regardless of the measurement instrument, the scattering parameters at zero frequency cannot be measured for practical reasons. At low frequencies, capacitive coupling effects lead to very high impedances and result in scattering parameters that cannot be distinguished from noise. Hence the measurement is performed down to the smallest available frequency. The data for the DC point is then extrapolated numerically.

Fig. 4 shows the s_{22} and s_{12} , which are the reflection and transmission coefficients of port 2, measured down to 10 Hz to capture any interesting behavior in low frequencies. The cable shows capacitive characteristics below 100 kHz.

The complete set of s-parameters can be used to build a model of the device. Agilent ADS was the software package used for this work. It allows scattering parameter measurements to be imported from the VNA and automatically builds a model that can be embedded in time and frequency domain simulations.

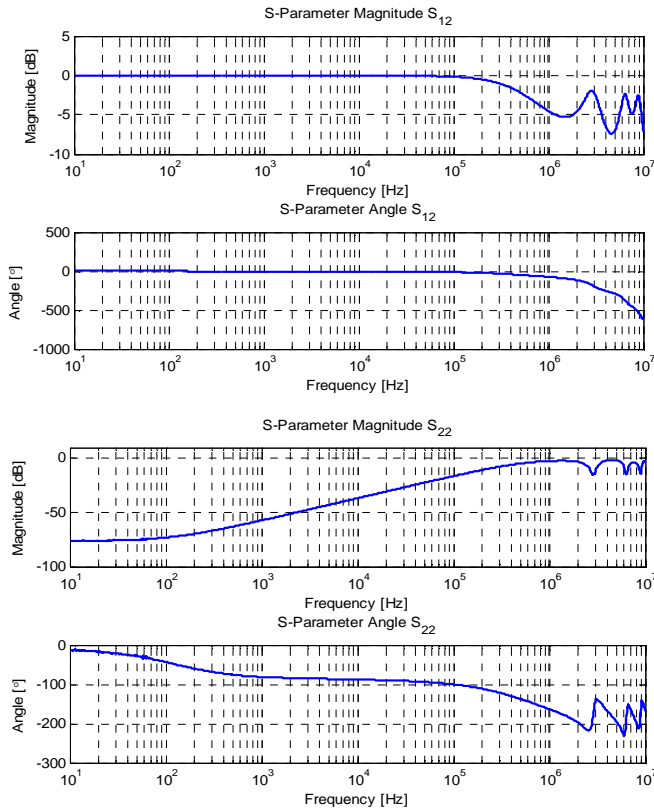


Fig. 4 s_{12} (the upper plot) and s_{22} (the lower plot) show the transmission between two sides of the center conductor of the cable and the reflection coefficient of port 2 respectively. It can be seen that for the frequencies up to 10 kHz, the center conductor can be assumed as a short circuit with lossless transmission (0 dB) and no phase shift.

III. TIME-DOMAIN VALIDATION

The authors suggest testing the validity and accuracy of the model before using it in grounding studies. Such validation can be accomplished by time domain analysis with a test signal. Typical test signals such as impulse signals and step responses cannot easily be applied to the cable due to the physical difficulties of generating clean test signals. The rising step function is hard to produce because of the capacitive nature of the cable, which would make the step response being dominated by the output impedance of the signal generator. However, the transient caused by a sudden short circuit can capture the characteristics of the system. In addition, this test resembles a ground fault scenario in which the voltage of one rail reaches zero (the ground voltage) in a very short time. Generating a fast, low impedance short is less challenging than producing a steep rising voltage.

To fulfill this need, a two-step test has been developed and implemented on a power cable. The first step of the test is to charge the cable to a certain known voltage level with respect to its shield via a charged capacitor. Then, the center conductor at the other end of the cable is shorted to the shield. This scenario will cause a voltage oscillation across the capacitor, which is recorded for evaluation. Even though the applied test voltages are very small compared to the operation voltage, the response is valid based on the assumption that the cable is a linear component in the voltage range of interest.

A. Electronic Circuit

Fig. 5 shows the test arrangement. The circuit must be simple enough to allow it to be simulated accurately. A polyester film capacitor has been used on one side of the cable since these types of capacitors have a very small equivalent series resistance (ESR), a low parasitic inductance (ESL), and are therefore very close to an ideal capacitor in the frequency range of interest. The capacitor is charged by two 9 V batteries in series using a resistor. The value of the resistor must be chosen large enough to decouple the battery from the rest of the setup and small enough to recharge the capacitor between the pulses. The value of 1 k Ω proved to be a good tradeoff for the chosen DUT. Since the transient response occurs in a time much shorter than the charging time, the presence of the battery cannot affect the transient response waveform considerably. Simulation confirmed that setting the initial voltage of the capacitor to 18 V and removing the battery instead of keeping the battery and the resistor in the model does not make a significant difference in the final result.

On the receiving side, an RF MOSFET is used as a switch. Having a very low on-state series resistance (13 m Ω) and a very small fall time (7 ns), makes this MOSFET very similar to an ideal switch. The other advantage of using a MOSFET is that the driving circuit behind the gate is isolated from the rest of the system and does not affect the dynamics of the cable. The circuit is powered by two 9 V batteries in series to keep the system ungrounded. When measuring the voltages at both sides using an oscilloscope, the probes have to be isolated to not introduce a common ground path. All connections between the components and also the component leads are kept as short as possible in order to avoid unwanted inductance. The pulse generator has a pulse repetition frequency of less than 200 Hz and a pulse length of 3 ms. The duty cycle of the timer circuit is set to allow the circuit to completely charge and discharge the capacitor.

The choice of an appropriate gate resistor is of utmost importance. It must allow a high rate of fall of voltage (dV/dt) without causing MOSFET internal oscillations. After a series of tests with different MOSFETs and gate resistors, an IPD160N04 MOSFET and a gate resistor of 2.5 Ω were chosen.

B. Validation of S-Parameter Model of a Distribution Cable

The voltage between the center conductor and the shield on the switch side (Fig. 5) had been measured to ensure that the voltage waveform is close to a perfect step function. It was noticed that the transient response is different when the scope is connected to both sides of the cable. Connecting both sides of the cable to the oscilloscope will make a ground loop consisting of the cable shield, the ground cables of the probes, and the ground plate of the oscilloscope. It will change the characteristics of the system as well as the response. The solution to this problem was to only measure the voltage on one side at a time to avoid having the ground loop.

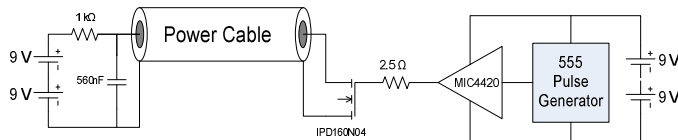


Fig. 5 A simplified graph of the validation test. The capacitor side is connected to a capacitor which is charged by the battery. On the fault side of the cable, an RF MOSFET simulates a fault by short circuiting the cable to ground with a negligible on-state series resistance. The MOSFET circuit is powered by two 9 V batteries in series that keeps the circuit ungrounded and separate from the capacitor side.

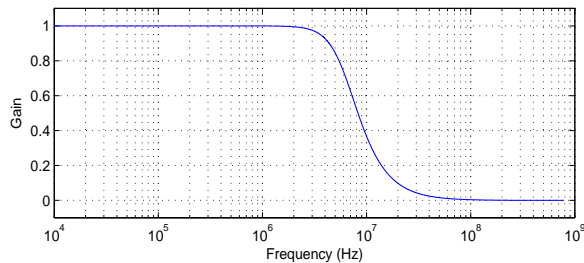


Fig. 6 The frequency response of the utilized 2nd order low pass Butterworth filter with a cutoff frequency of 1 MHz.

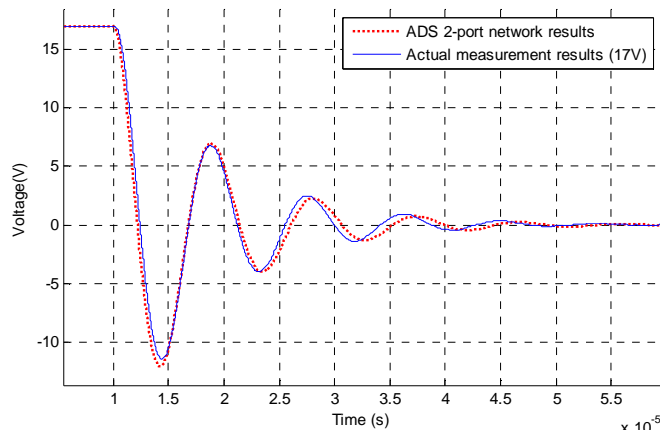


Fig. 7 The transient response of the cable. The solid blue line shows the time domain measurement filtered by low pass Butterworth filter, while the dotted red line is the output of the simulations.

The captured data from the scope contains noise and had to be filtered to have a smooth response. The cutoff frequency was chosen in a way that it completely passes the fundamental frequency of the transient response, which is around 110 kHz. The filter used to achieve this goal is a second order low pass Butterworth filter with a cutoff frequency of 1 MHz. It has to be noted that the filter phase shift at the fundamental frequency is less than 2 degrees, therefore negligible. The frequency response of this filter is shown in Fig. 6. The filtering approach is discussed in detail in [8].

Fig. 7 shows the comparison between the simulation results and the time domain measurements. The fundamental frequency is 107.5 kHz for the simulation result and 112 kHz for the experimental data. The peak voltage of the measured data in the first period of oscillations is 11.5 V and it is 0.65 V (5.6%) less than the peak value of the simulation output.

The total error consists of model errors and measurement errors. It is worth considering that the MOSFET switch was modeled by an ideal switch in series with a 13 mΩ resistor while neglecting the high frequency characteristics of the

MOSFET. The falling rate of the voltage across the MOSFET is limited by the dynamics of the MOSFET. Another source of error can be the oscilloscope probes used to capture the voltage waveforms. The probes were calibrated to rule out the effect of the input capacitance of the oscilloscope port. However, the inductance of the probe cable is not taken into account. It is worth noting that this inductance is negligible and cannot make a considerable difference in waveform. The range of influence of these error sources is under further investigation.

The simulation results shown in the introduction (Fig. 3) are based on the validated model of the power cable. This is an example of how a validated model with coupling to ground can be used to run power system simulations.

IV. CONCLUSION

An approach for validation of the scattering parameter based models for grounding studies of shipboard power systems has been introduced. The motivation for the approach has been explained. An example based on a distribution cable has been presented. The considerations and challenges in measuring the scattering parameters of the device under test and the time domain measurements have been discussed and addressed. The hardware used to capture the transient response of the system, except for the instruments such as the probes, the oscilloscope, and the VNA, has been described in detail. The result of the time domain measurement has been compared to the simulation output based on an S-parameter based model. The comparison shows that the model can appropriately predict the important characteristics of the transient response of the system such as the frequency and damping ratio with high accuracy.

The example of a distribution cable was chosen for its dominating impact to over voltages caused by ground faults, which comes from the parasitic coupling to ground. In future, this method is planned to be tested on other components of the shipboard power system such as power electronic converters and rotating machines.

ACKNOWLEDGMENT

The authors would like to thank the ESRDC (Electric Ship Research and Developing Consortium) Grounding Team for the many valuable discussions. This project is funded in part by the Office of Naval Research under grant No. N00014-04-1-0664.

REFERENCES

- [1] B. Jacobson, J. Walker, "Grounding Considerations for DC and Mixed DC and AC Power Systems," American Society of Naval Engineers, pp. 49-62, 2007.
- [2] J. Ciezki, D. Infante, L. Graber, S. Pekarek, and M. Steurer, "Evaluation of Rail Harmonics in Alternative MVDC Grounding Strategies," *ASNE Electric Machines Technologies Symposium (EMTS)*, Philadelphia, PA, 19-20 May 2010.
- [3] L. Graber, D. Infante, M. Steurer, and W.W. Brey, "Validation of cable models for simulation of transients in shipboard power systems," *IEEE International Conference on High Voltage Engineering and Application (ICHVE)*, New Orleans, LA, 10-14 October 2010.

- [4] L. Graber, D. Infante, M. Steurer, and W.W. Brey, "Model Validation for Shipboard Power Cables Using Scattering Parameters," *Journal of High Voltage Engineering*, Vol. 37, Issue 11 (2011).
- [5] L. Graber, M. Steurer, J. Kvitkovic, M. Kofler, S. Pekarek, R.A. Howard, A. Taher, M.S. Mazzola, and A.E. Card J.M., "Time and Frequency Domain Methods to Evaluate Grounding Strategies for Medium Voltage DC Shipboard Power Systems," *IEEE Electric Ship Technologies Symposium (ESTS)*, Arlington, VA, 21–21 April 2013.
- [6] D.M. Pozar, "Chapter 5: Microwave Network Analysis" in *Microwave Engineering*, Addison Wesley publishing company, pp. 220-230, 1990.
- [7] V. Cecchi, A. St.Leger, K. Miu, C.O. Nwankpa, "Modeling Approach for Transmission Lines in the Presence of Non-Fundamental Frequencies," *IEEE Transactions on Power Delivery*, vol. 24, no. 4, pp.2328-2335, Oct. 2009.
- [8] B. Butterworth, "On the Theory of Filter Amplifiers," *Experimental Wireless and the Wireless Engineer*, Vol. 7, 1930.

Behshad Mohebbali received his Bachelor of Science degree in electrical engineering in 2012 from Iran University of Science and Technology, Tehran. He had been working at Tida Pars Co. from 2010 to 2012 as design Engineer. He is currently pursuing a master of electrical engineering at Florida State University and is expecting to graduate in summer 2015. He has been working in the power systems group at Center for Advanced Power Systems since spring 2013 as a research assistant. His research interests are High frequency modeling of the Power system components and model validation.

Patrick Breslend completed his B.S. in electrical engineering in May of 2012 from Florida State University, Tallahassee, FL. He is now pursuing an M.S.E.E. degree from Florida State University under Dr. Mischa Steurer and Dr. Chris Edrington and is expected to finish July of 2014. He has worked at Florida State University's Center for Advanced Power Systems since 2009. His research includes power electronic based distribution systems, MVDC electric ship system modeling, and high frequency models based on scattering parameter measurements.

Lukas Graber received his PhD degree from ETH Zurich in 2010. Currently he is assistant scholar scientist at the Center for Advanced Power Systems (CAPS), Florida State University, working in the fields of cryogenic dielectrics and grounding of shipboard power systems. He is leading the High Voltage Laboratory at CAPS. Dr. Graber is senior member of IEEE, member of the Cryogenic Society of America (CSA), member of Electrosuisse, and contributes to the re-write of IEEE 45 "Recommended Practice for Electric Installations on Shipboard".

Michael "Mischa" Steurer received a Master of Electrical Engineering in 1995 from the Vienna University of Technology, Austria, and his Ph.D. in Technical Science in 2001 from the Swiss Federal Institute of Technology Zurich, Switzerland. Since then, Dr. Steurer leads the power systems group at the Florida State University (FSU) Center for Advanced Power Systems (CAPS) where he focusing on hardware-in-the-loop real-time simulation and modeling of integrated power systems for all-electric ships and future terrestrial power systems. He is a senior member of the IEEE and a member of CIGRE. Dr. Steurer is chairman of the IEEE Task Force on "Fault Current Limiter Testing", and contributes to several IEEE working groups and one CIGRE working group. Dr. Steurer has authored and co-authored more than 100 technical papers in the area of shipboard power systems, hardware-in-the-loop real-time simulation, and superconductivity.

APPENDIX C

Matthias Kofler & Dr. Lukas Graber
CENTER FOR ADVANCED POWER SYSTEMS (CAPS),
FLORIDA STATE UNIVERSITY

Richard A. Benson
MATHWORKS

Implementing S-parameter Models in MATLAB Simulink to Analyze Transients in Ungrounded Shipboard Power Systems

INTRODUCTION

The United States Navy is moving towards the next generation of surface combatant ships, based on the All-Electric Ship (AES) concept [1], [2]. This new class of naval ships employs new ship designs and has the ability to make use of advanced electric weaponry. The key feature of an AES is the employment of a next generation integrated power system (NGIPS) [3], [4], [1]. This architecture features electric propulsion and combines propulsion and electrical ship service system into a single power system [5], [2]. This scheme of power utilization and distribution throughout the ship offers benefits in many respects compared to conventional naval ships. Overall, it enables ship designers increased flexibility in ship design (re)configurability to meet the individual needs and operational requirements of different ship types [1], [6], [7]. However, this comes with a couple of challenges considering the complexity of the system, the high power density, and the requirements regarding robustness [6]. One essential area of research is on the design of appropriate power system architectures. As of today, the medium-voltage direct current (MVDC) integrated power system is a candidate for the NGIPS architecture, which can meet the high-power density requirements of future naval ships. It provides several advantages with regard to performance and total cost of ownership [7]. One important design aspect of MVDC shipboard power systems is grounding. The system grounding has significant impact to reliability and availability of power, survivability of impacts, continuity of service during faults, and personnel safety. Ungrounded (unintentionally grounded) and high impedance grounded systems generally allow continuity of operation in the presence of a single rail-to-ground fault [8]. On the negative side, studies show that voltage transients can be more severe than for (low impedance) grounded systems [9], [10]. Figure 1 shows an example of such voltage transients as they can occur. In order to study these transients, simulation models are required that correctly implement the coupling-to-ground of key components of the power system, including cables, bus bars, electric machinery, converters, and switchgear. In reality, things are even more complex: The electric potential of the ship hull is neither constant nor uniform, but is a function of ship hull currents.

In order to study ship hull currents, models for local coupling to the ship hull, along with an electric hull model, are required. The distributed nature of ship hull and power distribution system requires models beyond the limits of lumped element circuits. Similar situations are well known to designers of microwave circuits and antennas. Often, it can be assumed that these networks satisfy the criteria of

ABSTRACT

■ One area of ongoing research within the Electric Ship Research and Development Consortium (ESRDC) is ungrounded medium-voltage power systems operated at DC (MVDC). Special interest is in the simulation of high frequency transients on the DC distribution bus of shipboard power systems, as well as ship hull currents. Shipboard power systems of future all-electric ships are expected to exhibit high-power density, short line lengths, and low damping characteristics. The exact shape of these transients depends on high-frequency characteristics of all components, including the DC distribution bus and the coupling to the ship hull. For practical reasons, time domain simulations are typically lumped element models, which do not represent the distributed nature of the system to be modeled (e.g. wave propagation and reflection effects). In this paper, a frequency domain modeling approach based on the theory of scattering parameters (S-parameters) is proposed. A method on how to incorporate shipboard components is presented. It is based on Laplace domain transfer functions in linear multiport networks, characterized by their S-parameters into transient power systems simulations. The tool of choice is SimPowerSystems, a toolbox for MATLAB/Simulink numerical computing environment. The presented approach aims at complementing existing modeling techniques to ultimately increase the quality of simulation results. A rigorous validation based on computer models and experiments on power cables, followed by a discussion, completes this paper.

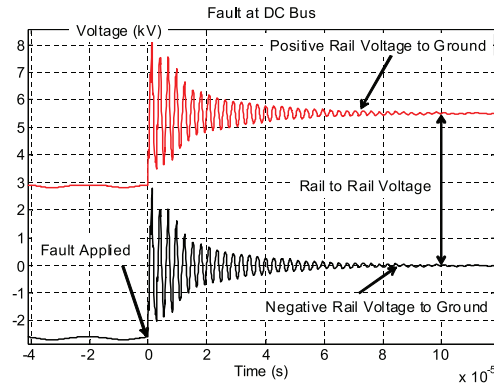


FIGURE 1. Transient phenomena and system offset for a high grounding impedance [10].

linearity and time invariance to allow use of linear network theory. In microwave engineering, most circuits are characterized by their scattering parameters (S-parameters). The concept of S-parameters has been introduced and initially used in the context of shipboard power systems at the Center for Advanced Power Systems (CAPS) in 2011 [11]. The subject of this past study was on the applicability of S-parameters for model validation, with focus on existing cable models, as in [12]. The next logical step is to directly introduce S-parameter models into shipboard power systems simulations.

S-parameter Models of Power Systems Components

S-parameters play an important role in microwave theory and provide an appropriate concept for modeling and characterization of linear electrical systems over a wide frequency range. A multiport network, as shown in Figure 2 (commonly termed as N-port) is an arbitrary electrical network that theoretically may have any number (N) of ports. A network port is understood as a pair of terminals.

In frequency domain, a linear multiport is generally described by its S-parameters, utilizing the theory of linear superposition and the matrix representation [14]

$$\mathbf{b} = \mathbf{S} \mathbf{a} \quad (1)$$

with \mathbf{a} and \mathbf{b} being the waves traveling toward and outward the network at all ports present, and \mathbf{S} denoting the scattering matrix (S-matrix). Thus, both \mathbf{a} and \mathbf{b} are vectors of dimension $N \times 1$, whereas \mathbf{S} is a $N \times N$ matrix containing

N^2 elements where N is the total number of network ports. Considering a single port of a N-port network, generally denoted as the i^{th} -port, a and b are defined in terms of the total voltage and current as

$$a_i = \frac{V_i + Z_i I_i}{2\sqrt{\text{Re}Z_i}} \quad (2)$$

$$b_i = \frac{V_i - Z_i I_i}{2\sqrt{\text{Re}Z_i}} \quad (3)$$

and known in literature as traveling waves [15]. V_i and I_i are the terminal voltage across and terminal current into the i^{th} -port. Z_i is the reference impedance of the corresponding port. The S-matrix describes the transmission and reflection characteristics of the network in terms of incident and reflected waves at all ports present [16]. All elements of the S-matrix

$$\mathbf{S} = (S_{ij})_{i,j=1,\dots,N}$$

are a function of frequency location of the reference or terminal planes t_i (define the network ports) and defined for steady-state stimuli in terms of a set of N reference impedances. Consequently, \mathbf{S} becomes a matrix $N \times N \times M$,

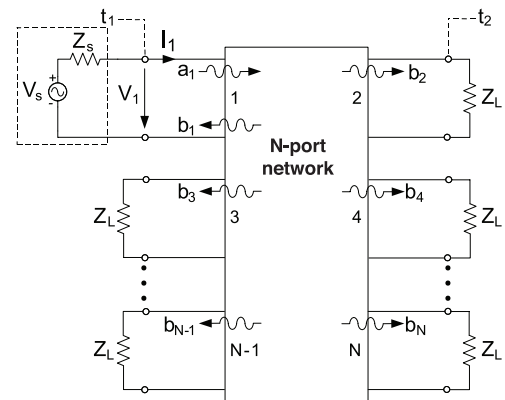


FIGURE 2. Arbitrary N-port network with a_i as the incident wave and b_i as the transmitted and reflected waves. V_s and Z_s are the source voltage and source impedance. Z_L is the port termination equal to the source impedance. V_i is the potential difference between the i^{th} -port and a reference (e.g., GND). I_i is the current through the interface of port i and the load or source. The reference planes are denoted as t_i [13].

representing MN -port S-parameters, where M is the total number of frequency points. The expressions (2) and (3) are defined for the use of a real-valued positive impedance Z_r . S-parameters are most commonly given with reference to a 50Ω test environment.

Considering S-parameters, each element of the main diagonal of \mathbf{S} is a reflection coefficient of a corresponding port when the other ports are terminated by perfect matched loads, and contains the ratio of amplitude of reflected and incident wave of a certain frequency [17]. Conversely, the off-diagonal elements are transmission coefficients between the ports containing the ratio of amplitude of transmitted and incident wave [17]. Thus, S-parameters can be determined by

$$s_{ij}(f) = \left. \frac{b_i}{a_j} \right|_{a_k=0} \quad (4)$$

The diagonal S-parameters are obtained for $i = j \forall k \neq i$ with b_i being the reflected power wave amplitude and a_i being the incident power wave amplitude at the i^{th} -port. The off-diagonal S-parameters can be found for $i \neq j \forall k \neq j$ with b_i being the transmitted power wave amplitude and a_i being the incident power wave amplitude at the j^{th} -port. The subscripted condition implies that no power waves are returned to the network from all other ports k , which are considered not being stimulated but to be connected to perfect matched loads. Following the S-parameter convention s_{ij} , the first subscript (i) always refers to the responding port, or in other words to the port at which the wave is traveling outward of the network. The second subscript (j) refers to the port toward which the wave is traveling. Various simulation software packages (e.g., MathWorks MATLAB® or Agilent Technologies Advanced Design System [ADS]) routinely used in the high-frequency engineering as well as finite element analysis software packages such as COMSOL Multiphysics®, permit the extraction and manipulation of network parameters such as Y , Z , and S-parameters of electrical networks in a relatively simple process. In practice, the S-parameters of the device under test (DUT) are typically measured by means of a vector network analyzer (VNA). As the DUT features a unique performance at a certain frequency

from one port to another, the S-parameters are determined in a certain frequency range of interest with a high density of frequency points (typically hundreds, or sometimes exceeding one thousand). Therefore, the VNA sweeps a sinusoidal electrical signal linearly or logarithmically through a user-specified frequency range that measures the magnitude and phase characteristics of reflected and transmitted signals. A complete sweep is usually just a matter of a few seconds or less, and directly measures the corresponding S-matrix at each frequency point. A calibration measurement allows for compensation of the effect of the leads to the DUT.

Model Implementation and Validation

A. MODEL IMPLEMENTATION

The implementation of a circuit level model from S-parameter measurements is accomplished in the MATLAB/Simulink [18] graphical programming environment with SimPowerSystems. The initial choice using this software package is based on availability and experience, as well as on the fact that this computing platform is commonly used in ESRDC activities for shipboard power systems simulations. The basic implementation consists of three distinct steps:

- fitting a rational function to the frequency domain S-parameters data
- compute the transfer function and build the rational model blocks for each S-parameter
- incorporate these blocks into a circuit level model.

1. Rational Function Fitting

The previous section has described how to obtain S-parameters of an N -port network. In order to use these data for simulation purposes, the complex frequency domain data have to be fitted. In the previous section, the lowercase “s” was used for S-parameters that might cause confusion in the Laplace domain in that the same character represents the complex frequency. For this reason, in this section S-parameters are indicated with an uppercase “S”. Referring to [19], [20], the objective of the fitting procedure (“rational fit”) is to create a mathematical model from the complex frequency domain data. Conceptually, this model would be a ratio of polynomials in the Laplace domain s . Following

this, a finite set of measured data (e.g., a single S-parameter) can be approximated by

$$S_{12}(s) = \frac{a_N s^N + a_{N-1} s^{N-1} + \dots + a_1 s + a_0}{b_M s^M + b_{M-1} s^{M-1} + \dots + b_1 s + b_0} \quad (5)$$

where $s = \sigma + j\omega$ is the complex frequency with $\omega = 2\pi f$. The polynomials involved with this approximation are typically of a high order (e.g., $M > 30$), and high frequencies are involved as well. When modeling high-speed serial data physical interconnects, the upper bounds of frequency are often well over 10 GHz. This creates a serious numerical challenge for the above formulation. The solution is to reformulate the problem into a more numerically friendly canonic form, a partial fraction expansion

$$S_{12}(s) = \sum_{m=1}^M \frac{c_m}{s - p_m} + d \quad (6)$$

where p_m are pole locations, c_m are the residues to the corresponding poles, and d is the direct feedthrough term that appears if $M=N$.

This approximation works well for lumped element systems that naturally have a finite order. However, the measurements have been made on distributed systems, which, in principle, have an infinite order. The distributed nature is due to the measurements being made on physically large elements that behave like transmission lines. One manifestation of this behavior is a time delay for end-to-end off-diagonal (transmission) measurements such as S_{12} and S_{21} that refer to a 2-port network. A small modification can be made to the partial fraction expansion to include the time delay, a so-termed modified rational function

$$S_{12}(s) = \left(\sum_{m=1}^M \frac{c_m}{s - p_m} + d \right) e^{-s\tau} \quad (7)$$

where τ is a coarse estimate of the time delay. Including this delay term can significantly reduce the order (M) required to achieve an accurate model. Furthermore, the model runs faster without compromising accuracy. The parameters of the fitting routine are fairly straightforward, and for the most part the user simply sets the desired fitting tolerance and the percentage of the calculated delay (obtained from the phase curve of the measured data) that is to be accounted for

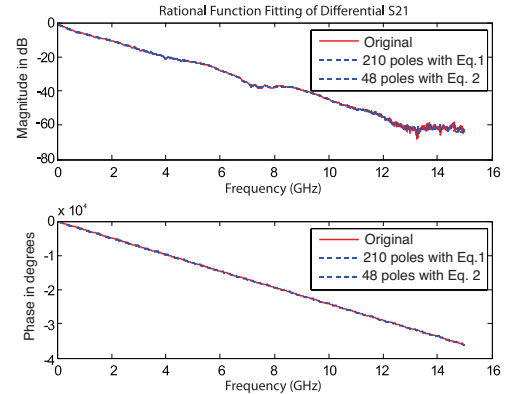


FIGURE 3. Comparison between the frequency response of the rational function object and that of the original data with equations (6) and (7) [19].

in the delay parameter. One can also stipulate the number of poles (and zeros) to be used, but it is typically simpler to specify a desired tolerance and let the fitting algorithm determine the required order of the system. In order to verify the accuracy of the model, one must evaluate the magnitude and phase response of the model from DC ($s=0$) through the frequency range of the measurement data and beyond and compare this to the measurement data. Figure 3 shows the results for a 210-pole model without delay term (Eq. 6) along with a 48-pole model with delay term (Eq. 7).

The fitting technique forces the phase to be zero at $s=0$ and can be adapted to assume a roll-off at the high frequency end. According to [21], [19], the modified rational function fitting has the following advantages compared to traditional techniques, such as inverse fast Fourier transform (IFFT):

- It provides the same level of accuracy as the IFFT method, with a model that is one or two orders of magnitude simpler.
- Model order reduction can be used to trade off complexity and accuracy through the use of fitting parameters.
- Typical VNA data have a low frequency cut-off, thus an extrapolation to DC is needed. Rational function models represent a physical transmission line and inherently constrain the phase to be zero at extrapolation to DC. Standard IFFT techniques do not prevent the extrapolated phase from being non-zero (corresponds to a non-physical delay). IFFT models require elaborate constraint

algorithms in order to force the extrapolated phase to zero at DC.

The presented technique relies on vector fitting. References [20] and [19] cover the applied fitting algorithm in more detail.

2. Generation of Transfer Function Blocks

Once the poles, residues, order, and time delay are verified, a Simulink model that implements the modified rational function (Eq. 7) can be created. Since the system being modeled is a real physical system, the input and output are naturally real numbers. The poles therefore naturally occur in complex conjugate pairs. These pairs can be combined into second order transfer function blocks. Non-complex real poles on the negative real axis of the s-plane can be included as single pole transfer function blocks. A typical rational model in Simulink is as shown in Figure 4.

As described above, the transfer function blocks (“stages” in Figure 4) are of second and first order. They implement the complex conjugate pole pairs and real poles and the corresponding residues, respectively. Note that each transfer function block always has real coefficients. This is why the poles and corresponding residues of the rational function object of each S-parameter need to be converted into real numerators and denominators for use in the Laplace transform

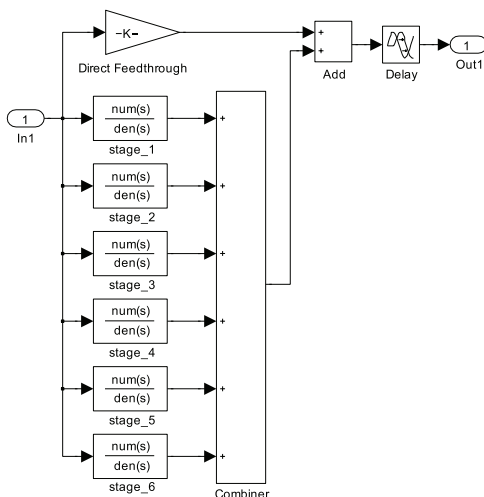


FIGURE 4. Simulink model of a rational function object representing a single S-parameter.

transfer function blocks. Figure 4 shows a relatively low order model compared to that which real-world measurement data require. However, even this low order model would be very tedious and error prone to create manually. Fortunately, MATLAB allows the capability to automatically build and modify a Simulink model purely from MATLAB code without using the Simulink user interface. This can be achieved using MATLAB-Simulink API (application program interface) commands, which enables the option to make the construction of far more complex (higher order) models virtually effortless.

3. Circuit Level Model Implementation

This discussion is continued on a 2-port example. The proposed approach can be easily extended to N ports, which allow the study of many of the most common components of a 3-phase power system (e.g., $N=6$). The final step in the modeling process is to include the 4 rational transfer function blocks in a circuit level environment. SimPowerSystems, a toolbox for Simulink, is optimized for the needs of a power systems engineer to model power systems. However, the toolbox does not natively support S-parameters, but it can be extended to do so by using controlled sources and measurements of both voltage and current. From a “top level”, the S-parameter model looks as shown in Figure 5.

The interface between the unidirectional signal domain of Simulink and the circuit domain of SimPowerSystems is accomplished with the “Vin” block (a controlled voltage source) and the “VML” block measuring the voltage across the load “Zl” and producing a signal labeled “Vout”. More complex passive and active sources and loads could be incorporated around the S-parameter

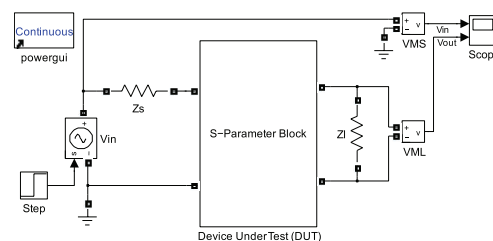


FIGURE 5. S-parameter model block built in Simulink/SimPowerSystems. Any complex passive and active sources and loads can be incorporated around the S-parameters model block.

model block. The internals of the S-parameter block are shown in Figure 6. The four blocks in the central portion of the subsystem are the rational fit transfer function elements. The model is based on equations 1-3. As a final note on the modeling topic, the underlying computational Simulink engine is a variable-step Ordinary Differential Equation (ODE) solver. In order to solve the model, the SimPowerSystems engine maps the circuit level description into a state space format that can be simulated with an ODE solver.

This can often lead to so-called “algebraic loops” which are difficult to solve numerically. However, the Simulink engine has been optimized over many years to efficiently handle this computational challenge by providing a comprehensive set of equations and systems solvers. Adding time delay blocks with a very small time constant in the S-parameter model (between “Add” and “V1” as well as “Add3” and “V2”) can break algebraic loops and make the simulation run considerably faster. Simulation performances have shown that the accuracy of the numerical simulation results, as well as the simulation speed, strongly depend on solver settings. Improper solver settings significantly slow down the simulation and may lead to inaccurate results. In the worst case, this can result in algebraic loop(s) that cannot be solved by MATLAB/Simulink. Table 1 shows the solver settings found to work very well for the simulations performed. Note, these settings serve as a starting point and will need to be adjusted on a case-by-case basis depending on the bandwidth of the system being modeled. MATLAB/Simulink version 7.9.1/7.4.1 (MATLAB R2009b SP1) was used. However,

CONFIG. PARAMETERS	SETTINGS 1	SETTINGS 2
Type	Variable-Step	Variable-Step
Solver	ode23tb (stiff/TR-BDF2)	ode15s (stiff/NDF)
Initial Step Size	auto	1e-11
Min Step Size	auto	auto
Max Step Size	1e-9	1e-7
Relative Tolerance	1e-3	1e-4
Absolute Tolerance	auto	1e-4
Solver Reset Method	Robust	Fast
Algorithm	Nonadaptive	Nonadaptive

TABLE 1. Solver settings used for the simulations performed in Simulink/SimPowerSystems. All other settings other than those stated here were left at default values (default settings depend on solver type).

the solver settings should not depend on the version of MATLAB.

B. MODEL VALIDATION

The model validation was conducted in two steps. In a first step (“computer model-based validation”), artificially generated S-parameters from a lumped element circuit model were used. This approach excluded typical error sources of experimental validation such as noise, distortion, and parasitic capacitance and inductance of various components in the circuit. The second validation step (“experimental validation”) was based on an experiment with a power distribution cable as it

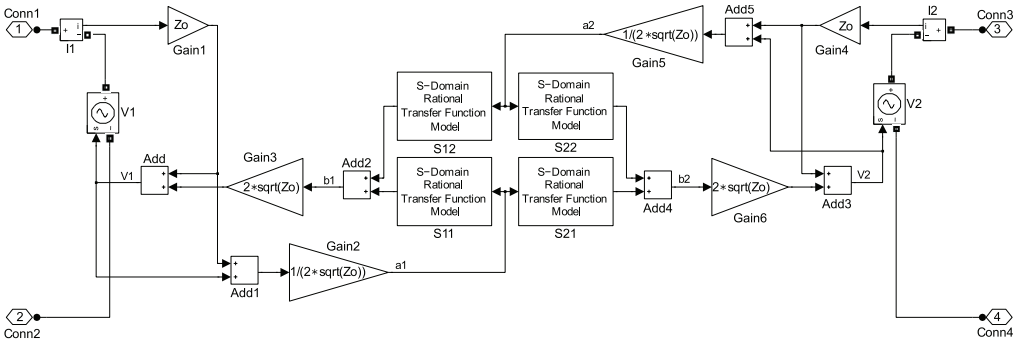


FIGURE 6. Internals of the 2-port S-parameters model block that implements the equations that link the four S-parameters to the input and output port voltage and current.

was used in [11]. S-parameters were measured by a vector network analyzer.

1. Computer Model-Based Validation

The validation of the implementation described in the previous section has been conducted using the RF simulation package ADS (Ver. 2011.10 [22]). The initial choice for using this software package is based on the fact that it is routinely used for high-frequency and microwave electronics for circuit analysis and design. ADS allows for easy extraction of S-parameters from such circuits and to write the set of data into the Touchstone data file format. Equally important, it allows implementation of S-parameters based on Touchstone files by means of S-parameter blocks available in the component library. As can be seen in Figure 7, a linear time-invariant (LTI) network has been defined by a circuit using passive lumped elements. The output of certain input excitation (step function) was recorded. Recording the step response is reasonable since the step function: a) may be considered as system fault initiation and b) enables the evaluation over a wide range of the frequency spectrum in which voltage transients may be present. The circuit built consists of two π transmission line models representing two single-phase transmission lines. A π -line model for a short section of transmission line is composed of a capacitor C coupling the signal to ground, followed by a series inductance L and resistance R , followed by another capacitor C coupling to ground. The resistor in series with the inductance represents the power loss. The two π -segments are cross-coupled by two capacitors (C_g , C_o) that lead to a 4-port network configuration. Subsequently, the extracted set of S-parameters have been used to implement the network in Simulink/SimPowerSystems based on the S-parameter implementation approach described. For comparison purposes, the same S-parameters have been implemented in ADS using the 4-port S-parameter block natively available. Figure 8 shows an overlay of the simulation results. As can be seen, the output voltages of the S-parameter model in Simulink/SimPowerSystems are virtually identical with the output voltages of the lumped element model, as well as identical with the model based on the S-parameter data

of the Touchstone data file. The latter are both implemented in ADS. The Touchstone data file generated includes the S-parameters data from 1 Hz to 250 MHz. In order to correctly simulate a step response, the DC point is needed. This is why ADS performs an extrapolation down to 0 Hz, which introduces a certain level of error. The “ringing” at approximately 4 μ s in the ADS simulation using S-parameter data is a result of truncating the frequency response and ADS impulse response calculations [23].

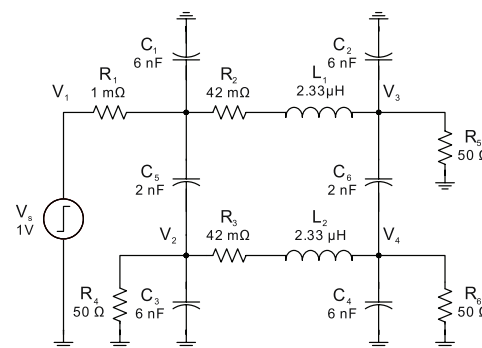


FIGURE 7. Computer Model-based Validation Circuit designed in ADS. Two π -sections representing two single-phase transmission lines. Those are cross-coupled by two capacitors that lead to a 4-port network configuration.

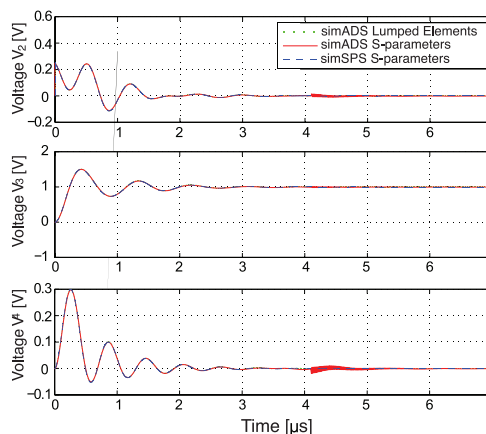


FIGURE 8. Step response of the 4-port network used for the validation process. The red and blue traces represent the output voltages of the numerical S-parameters modeling simulation in MATLAB/Simulink and ADS respectively. The green trace corresponds to the lumped element case (almost not visible because of perfect match with the result out of MATLAB/Simulink).

2. Experimental Validation

The purpose of this validation is to compare the results from the model with the results obtained from the experiment setup shown in Figure 9. For this purpose, a capacitor with low equivalent series resistance (ESR) connected to the cable will be charged to a constant DC voltage. The other end of the cable was short-circuited to its shield at a certain instant of time. To get the most reliable results, the following considerations were taken into account:

- A mechanical switch was used to short-circuit the cable end. This kind of switch showed bouncing characteristics in the moment of switching, resulting in a non-zero voltage across its contacts. This can be compensated by feeding back the voltage to the circuit simulation. The switch was later replaced by a MOSFET.
- The circuit was designed for minimum stray capacitances and inductances. All interconnects are kept short. Figure 9 shows the components used for the experiment. Note that the length of leads to the battery is not critical since it is decoupled by the charging resistor.
- The impact of the probes used (1:10, 10 M Ω ||16 pF compensated) was compensated by modeling them in the circuit simulation.

Figure 11 shows the circuit model in the MATLAB/Simulink environment. The S-parameter block holds the S-parameters of the cable. R_p and C_p are the components used to model the probe of the oscilloscope. Resistor R_2 is introduced for numerical reasons. Its effect is negligible since its resistance is 10 $\mu\Omega$ only. As can be seen in Figure 10, the transient response of the model is similar to the measured transient. However, there is substantial difference in the frequency of the decaying oscillations. Figure 10 shows that the oscillation frequency of the model output is slightly larger ($\sim 4.5\%$) than the one of the data obtained from the experiment. The cause for this inaccuracy is the subject of ongoing investigations. The non-linear junction capacitance of the chosen power MOSFET, which is currently not included in the model, could be a contributing factor to the slight mismatch. Enough time should be given to the model to reach the steady state before short-circuiting the end of the cable.

Therefore, 20 μs were added at the beginning of the simulation. In order to calculate the frequency, the time distance between the first two minimums was considered as the period of the oscillations, respectively.

Outlook: Applicability to Power Systems

Components Other Than Cables and Bus Bars

Past studies in the Electric Ship Research and Development Consortium (ESRDC) [24], [25] have shown that power distribution cables have substantial impact to high frequency transients and coupling to ground characteristics in shipboard power systems. Models have indicated that power electronics devices (PED) and rotating machinery (e.g., turbo generators, propulsion motors) on the AES also have an impact to transients and ship hull currents, but typically to a lesser extent. Even so, future grounding studies are expected to include PEDs and rotating machinery. The block diagram in Figure 12 shows a generic shipboard power system. Each block represents a subsystem with its proper coupling to a specific location of the ship hull (bottom). It is not always obvious which of these subsystems would satisfy the LTI criterion and could therefore be modeled

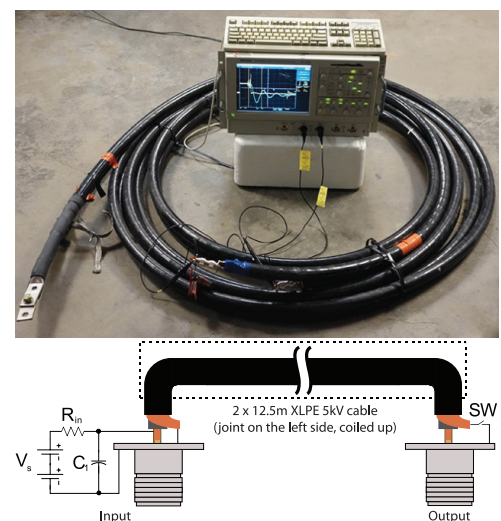


FIGURE 9. (Above) Setup used to perform an experimental validation. Basically, it consists of a 4-port VNA (Agilent E5071C), function generator (33220A) and the DUT (5kV XPLE power cable). (Below) RF connectors (Type N-connectors) are mounted on both ends of the cable. The switch "SW" is realized by means of a power MOSFET IRF2807.

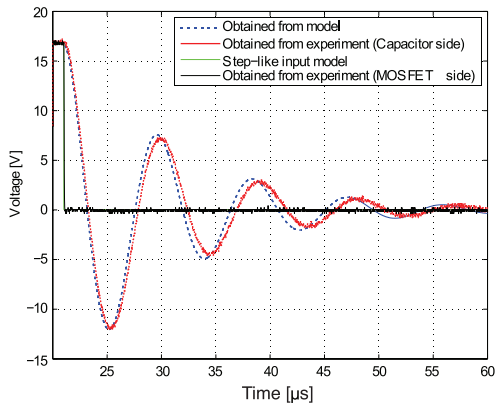


FIGURE 10. Step response of the 4-port network used for the validation process. The red and blue traces represent the output voltages of the numerical S-parameters modeling simulation in MATLAB/Simulink and ADS respectively. The green trace corresponds to the lumped element case (almost not visible because of perfect match with the result out of MATLAB/Simulink).

by S-parameters. Current efforts focus on the ship hull model, which definitely satisfies the LTI criterion, and the propulsion motor. First indications based on small scale laboratory experiments of motors in the 300 W range show that LTI methods can be applied to such motors. Further effort is required to determine whether the LTI assumption and, consequently, the concept of S-parameters can be applied to PED coupling to ground.

CONCLUSION

Shipboard power systems consist of multiple interacting components with specific characteristics regarding coupling to ground.

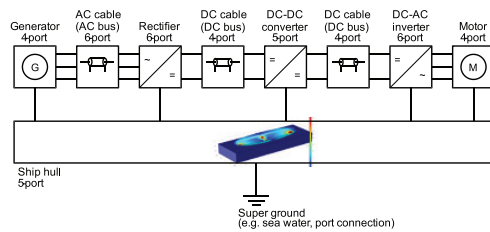


FIGURE 12. Simplified model of DC power distribution. Each block represents a linear time-invariant (LTI) network defined by S-parameters. Presence of the metallic ship hull results in a multi-port network. Each block is grounded by a local connection to the ship hull. The ship hull assumes ground potential at a single location only ("super ground").

Advanced numerical computer-based simulation models need to be developed which allow an accurate modeling of the characteristics of onboard integrated power system components. This includes the need to fully cover the coupling to ground effects to accurately study fault scenarios. In this work, a novel approach based on S-parameters has been developed and introduced for transient power systems modeling. It enables the capability to study alternative grounding methods with respect to different key characteristics, such as fault performance, ship hull currents, and electromagnetic interference (EMI) prediction/mitigation. Here, special focus was given to MVDC shipboard power system and its transient behavior of the DC bus in the event of a system fault. A method has been proposed to incorporate S-parameters in the MATLAB/Simulink environment. An S-parameter block was built for the MATLAB/Simulink technical computing environment, which is widely used

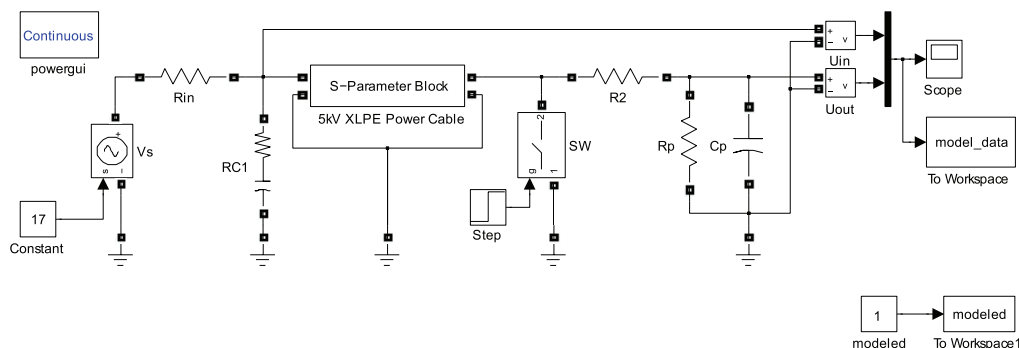


FIGURE 11. Experiment results compared to the model output. This set of data is obtained using a input voltage $V_s=17$ V.

to study the performance of shipboard power systems. It is assumed that the implementation method is suitable for other software packages used in power systems engineering (e.g., PSCAD®/EMTDC). Computer-based validation based on step response, as well as validation on the basis of experimental assembly, has been conducted. It has been shown that the technique proposed here is accurate, valuable, and feasible for high-fidelity transient power system

simulations. Overall, the S-parameter approach shows the potential to increase the quality of numerical computer-based simulation models by embedding the frequency, depending on the distributed nature of system components. It also allows the study of hull currents in the grounding system. Furthermore, it is conceivable that this procedure may serve as a tool for manufacturers to set specifications for equipment on a ship.

ACKNOWLEDGMENT

The authors would like to express their gratitude to Dr. William W. Brey from the National High Magnetic Field Laboratory (NHMFL) for his advice, and for letting us use NHMFL's network analyzers. We would also like to thank to collaborating researchers within ESRDC, namely Dr. Michael Steurer (Florida State University), Dr. Steven Pekarek (Purdue University), Dr. Michael Mazzola, and Ms. Angela Card (both Mississippi State University). They contributed valuable discussions and hardware. Special thanks goes to Mr. Behshad Mohebbi and Mr. Patrick Breslend (both Florida State University) for their help with the model validation. This project is sponsored by the Office of Naval Research ONR as part of the Electric Ship Research and Development Consortium ESRDC.

REFERENCES

- [1] V. R. Basam and A. Das. (2010) All Electric Ship-The Super Platform for Tomorrow's Naval Warfare. Second International Seminar and Exhibition on Naval Armaments. [Online]. Available: http://www.researchgate.net/publication/209434238_All_Electric_Ship_-_The_Super_Platform_for_Tomorrow's_Naval_Warfare [Accessed: July 14, 2013]
- [2] B. Wagner. (Nov. 2007) All-Electric Ship Could Begin to Take Shape By 2012. National Defense Magazine Archive. [Online]. Available: <http://www.nationaldefensemagazine.org/archive/2007/November/Pages/All-Electric2453.aspx> [Accessed: July 14, 2013]
- [3] Capt. N. Doerry. Open Architecture Approach for the Next Generation Integrated Power System. [Online]. Available: <https://www.navalengineers.org/SiteCollectionDocuments/2007%20Proceedings%20Documents/Automation%20and%20Controls%202007/1-2-9%20Paper.pdf> [Accessed: July 14, 2013]
- [4] L. HanYu and M. LongHua, "Integrated Protection on Shipboard Integrated Power System," International Conference on Advanced Power System Automation and Protection (APAP), vol. 1, pp. 252–255, 16–20 Oct. 2011.
- [5] N. H. Doerry and J. C. Davis. (May 1994) Integrated Power System for Marine Applications. Naval Engineers Journal. [Online]. Available: <http://www.doerry.org/norbert/papers/ASNE1994DoerryAndDavis.pdf> [Accessed: July 14, 2013]
- [6] K. P. Logan, "Intelligent Diagnostic Requirements of Future All-Electric Ship Integrated Power System," Industry Applications Society 52nd Annual Petroleum and Chemical Industry Conference, pp. 151–163, 12–14 Sep. 2005.
- [7] N. Doerry. (2009) Next Generation Integrated Power Systems for the Future Fleet. [Online]. Available: <http://www.doerry.org/norbert/papers/090106usna-ngips-nal.pdf> [Accessed: July 14, 2013]
- [8] Y. Pan, P. M. Silveira, M. Steurer, T. L. Baldwin, and P. F. Ribeiro, "A Fault Location Approach for High-Impedance Grounded DC Shipboard Power Distribution Systems," IEEE Power and Energy Society General Meeting -Conversion and Delivery of Electrical Energy in the 21st Century, no. 1-6, 20–24 Jul. 2008.
- [9] B. Jacobson and J. Walker, "Grounding Considerations for DC and Mixed DC and AC Power Systems," Society of Naval Engineers Journal, vol. 119, no. 2, pp. 49–62, Oct. 2007.
- [10] D. Lee, D. Infante, J. Langston, S. V. Poroseva, M. Steurer, and T. Baldwin, "Grounding Studies in a Medium Voltage DC Shipboard Power System with Uncertain Parameters," Conference on Grand Challenges in Modeling & Simulation, pp. 113–120, 2010.
- [11] L. Graber, D. Infante, M. Steurer, and W. W. Brey, "Model Validation for Shipboard Power Cables Using Scattering Parameters," High Voltage Engineering, vol. 37, no. 11, pp. 2836–2842, 2011.

- [12] V. Cecchi, A. Leger, and K. Miu, "Modeling Approach for Transmission Lines in the Presence of Non-Fundamental Frequencies," *IEEE Transactions on Power Delivery*, vol. 24, no. 4, pp. 2328–2335, Oct. 2009.
- [13] M. Kofler, "Scattering Parameters for Transient Analysis of Shipboard Power Systems," Master's thesis, University of Applied Sciences Upper Austria, 2013.
- [14] E. W. Matthews, "The Use of Scattering Matrices in Microwave Circuits," *IRE Transactions on Microwave Theory and Techniques*, vol. 3, no. 3, pp. 21–26, Apr. 1955.
- [15] K. Kurokawa, "Power Waves and the Scattering Matrix," *IEEE Transactions on Microwave Theory and Techniques*, vol. 13, no. 2, pp. 194–202, Mar. 1965.
- [16] D. M. Pozar, *Microwave and RF Design of Wireless Systems*. New York and Chichester: Wiley, 2000.
- [17] L. G. Maloratsky, *Passive RF & Microwave Integrated Circuits*. Amsterdam and Boston: Elsevier/Newnes, 2004.
- [18] The MathWorks Inc. Matlab 7.9.1 Service Pack 1 (R2009b SP1). (2009). [Online]. Available: <http://www.mathworks.com> [Accessed: July 14, 2013]
- [19] R. X. Zeng and J. H. Sinsky, "Modified Rational Function Modeling Technique for High Speed Circuits," *IEEE MTT-S Int. Microwave Symposium Digest*, pp. 1951–1954, 11–16 Jun. 2006.
- [20] B. Gustavsen and A. Semlyen, "Rational Approximation of Frequency Domain Responses by Vector Fitting," *IEEE Transactions Power Delivery*, vol. 14, no. 3, pp. 1051–1061, Jul 1999.
- [21] C. Warwick. (August 2007) Using model-based design in signal integrity engineering. *EE Times-India*. [Online]. Available: http://www.eetindia.co.in/STATIC/PDF/200708/EEIOL_2007AUG01_RFD_EDA_EMS_NETD_SIG_TA_01.pdf?SOURCES=DOWNLOAD [Accessed: July 14, 2013]
- [22] Agilent Design Software ADS 2011.10. (2011). [Online]. Available: <http://www.home.agilent.com/agilent/software.jsp?ckey=2212036&lc=eng&cc=US&nid=-34335.0&id=2212036&pageMode=Pv> [Accessed: July 14, 2013].
- [23] W. Rivas-Torres. Agilent Technologies, Inc. Email Correspondence 19 September 2012 (CaseID 1049432).
- [24] D. Infante, "Guiding the Selection of Physical Experiments for the Validation of a Model Designed to Study Grounding in DC Distribution Systems," Master's thesis, Florida State University, 2011.
- [25] D. Infante, J. Langston, L. Graber, and M. Steurer, "Guiding the Selection of Physical Experiments Supporting Validation of Electric Power System Models," *Conference on Grand Challenges in Modeling & Simulation*, pp. 173–180, 2011.

AUTHOR BIOGRAPHIES

MATTHIAS KOFLER was born in Innsbruck, Austria, in 1987. He received his B.Sc. and M.Sc. degree in automation engineering from University of Applied Sciences Upper Austria in 2010 and 2013, respectively. Since 2012, he has been a visiting master student at the Center for Advanced Power Systems (CAPS), Florida State University, working on grounding issues related to shipboard power systems.

RICHARD A. BENSON received his B.Sc. degree in electrical engineering with honors in 1971 from Northeastern University, Boston, MA. In 1973, he earned the M.Sc. from Northeastern as well. He started his career in 1966 as a co-op student working for General Radio (Concord, MA) and was hired as a development engineer in 1971. From there, he headed west to Northern California and continued to work for GR. In 1984, he left to co-found a small test and measurement company that was subsequently acquired by Tektronix. In 1985, he was exposed to MATLAB, and has been an ardent user ever since. After Tektronix, he co-founded another startup that was acquired by DSP Technology. In 2001, he joined MathWorks as a Consulting Applications Engineer stationed in Saratoga, CA. He is a Life Member of IEEE.

DR. LUKAS GRABER was born in Basel, Switzerland in 1976. He received the degree of doctor of science from ETH Zurich in 2010. Currently, he is an assistant scholar scientist at the Center for Advanced Power Systems (CAPS), Florida State University, working in the field of cryogenic dielectrics and grounding of shipboard power systems. He is leading the High Voltage Laboratory at CAPS. Dr. Graber is senior member of IEEE, a member of the Cryogenic Society of America (CSA), a member of Electrosuisse, and contributes to the re-write of IEEE 45 "Recommended Practice for Electric Installations on Shipboard." He is a Senior Member of IEEE.

APPENDIX D

Challenges of frequency domain measurement for modeling the components of shipboard power systems

Introduction

The choice of the grounding strategy for shipboard power systems of future all-electric ships has profound influence on the transient behavior of the system in case of ground faults. An important aspect that is taken into account in designing the power system is continuity of service in faulted state. Therefore, a solid connection to ground is not necessarily the best option for shipboard power systems with AC and DC zones as it is studied by *Jacobson & Walker (2007)*. Although the preferred strategy is to design the system ungrounded, or grounded via a high impedance connection, no shipboard power system can be considered completely ungrounded since there is always some level of capacitive coupling between the power system and the ship hull. The power range of the system can exceed 100 MW and necessitates having low resistance in the distribution rails or cables. Considering the relatively short length of the lines, line inductances are small compared to terrestrial power distribution systems. The combination of the aforementioned conditions, low line impedance and the parasitic capacitance coupling to the ship hull, suggests that high frequency transients with small damping ratio should be expected in ground fault scenarios.

There is a need to develop dedicated models that can predict the transient response of the ungrounded power systems to different fault scenarios with sufficient accuracy. These models must be able to be implemented for a variety of power system components seen onboard a ship. Furthermore, they must capture the common mode characteristics of components, such as power lines, rotating machines, and power converters and drives, as well as their high frequency features. In an early modeling effort, the parasitic coupling was approximated by capacitive elements to ground by *Ciecki et al. (May 2010)*. In the next step, a frequency domain approach was used to validate the linear lumped element models of power cables in *Graber et al. (October 2010; November 2011; April 2013)* scattering parameters were directly used for modeling purpose based on the assumption that the ground coupling can be modeled by linear time-invariant network parameters. The developed model was validated by a time domain approach resembling a ground fault in *Mohebbali et al. (2014)*.

There are basically two methods to obtain the necessary data for the aforementioned approach: The parameters can be calculated via finite element analysis (FEA) algorithms or they can be measured; the latter by either a Vector Network Analyzer (VNA), or an Impedance Analyzer (IA). Scattering and impedance parameters are widely used to characterize linear time-invariant networks. In spite of numerous advantages of FEA methods, which are not in the scope of this paper, measurement is still a powerful tool to capture the network parameters. This article attempts to comprehensively describe the procedure to performing scattering parameters measurement on the major components of a shipboard power system.

Characterization using a network analyzer

A Vector Network Analyzer (VNA) is an n -port device that can measure the scattering parameters of an m -port linear network by sending power signals at known frequencies into the

network under test from one port and calculating the ratio of the power level of the received signal to the input signal at all other ports (transmission parameters) as well as the ratio of the signal reflected to the port from which the original test signal has been sent out to the input signal (reflection parameters). n can be any number but most common are 2-port and 4-port VNAs. The power level of the test signal can be defined by the operator. Its range is different in different VNAs but typically it can be set between -50 dBm to $+10$ dBm. This is important if the device under test has some active or sensitive parts with input power limits. The incoming signal at each port is picked up by a directional coupler at that port. In order to eliminate noise, the received signal is filtered via a tunable band-pass filter. The bandwidth of the filter can be adjusted to balance accuracy of the measurement with time required for the measurement.

Theoretically, the impedance measurement and the scattering parameter measurement have no advantage over each other since the output data, i.e. the impedance matrix and the scattering matrix respectively, can be easily converted to the respective other matrix. However, while measuring the parameters of a multiport network is an ordinary task for a VNA, there is no standard method for measuring the impedance parameters of such networks using an impedance analyzer. In addition, the frequency range that typical VNAs offer is in most cases wider than the frequency range of a typical impedance analyzer. However, the frequency range in which the measurement outcome can be trusted depends highly on the auxiliary components such as the leads from the VNA to the device under test, the connectors, and the matched load resistors utilized to terminate the unused ports. The systematic error caused by the cables can be compensated by using the SOLT method, which stands for short, open, load, through. In the correction process the end of the cables connected to the VNA ports are terminated by known standard terminations, like a short circuit, an open circuit, and a load which is usually a precise $50\ \Omega$ over a wide frequency range, and also a through connection. By doing this, the error from the attenuation in the leads, or phase change along the leads, will be taken into account. The details about the error correction procedure of each VNA, often mistakenly called “calibration”, are elaborated in the user manual of the device.

There are several important considerations for highly accurate measurements:

1. The measurement leads to the device under test (DUT) has an impact to the upper frequency limit: There is no standard $50\ \Omega$ connection port on power system components. The VNA leads cannot be directly connected to the DUT terminals. Therefore, a pair of clamps for each port has to be used, which connects the DUT terminal and its ground to the center conductor and the shield of the VNA cable, respectively as shown in Figure 1. A 50 cm long wire connects each clamp to the N-connector connected to the VNA cable. The aforesaid setup shows changes in the measurement in high frequency range when the clamps are held in extreme positions, which were the furthest and the nearest distance from each other as shown in Figure 2. By doing the extreme position test, one can determine the upper frequency limit, which is well below the lowest frequency impacted by the layout of the leads.
2. The choice and number of ports: The choice of the number and the location of the ports depend on the application in which the measured data is going to be utilized. In cases where the DUT has more ports than the VNA, matched load resistors used to terminate the unused ports add systematic error due to their non-ideal frequency characteristics. In case of having an n port VNA, a k port network would need $k-n$ Termination resistor in each round of measurement. The number of ports and their location must be chosen according to the needs

of the application. A terminal which is not being used in the modeling and simulation can be ignored in the measurement process. A practical example for this case is the neutral point of rotating machines, which is discussed in detail in *Breslend et al. (September 2014)*.

3. Lower frequency limit: Because of the capacitive characteristics of the ground coupling in lower frequencies, the reflection parameters (the diagonal components of the S matrix) show resemblance to the corresponding scattering parameters of an ideal capacitor. It means as the frequency approaches DC point, the S-parameter value drops. The parameter that limits the minimum measurable frequency is the noise floor, as it can be seen in Figure 3 in frequencies below 1 kHz. The lower frequency limit has to be set high enough to prevent the reflection parameters from hitting the noise floor. In order to find such a frequency the measurement has to start from a very low frequency but a specific number of starting points may be cut out before putting the data into a model.
4. Intermediate frequency bandwidth: The intermediate frequency (IF) bandwidth is the adjustable bandwidth of the tunable input band-pass filter. Having a narrower bandwidth means that each single measurement point on the frequency range would take longer to be done. On the other hand, a wide bandwidth might be problematic in the low frequencies. The maximum value IF bandwidth which can give a reliable result is half of the smallest frequency in which the measurement is done.



Fig. 1 The connection between the DUT (2.5 MW rotating machine on the left and helium gas cooled superconducting cable on the right) and the VNA.

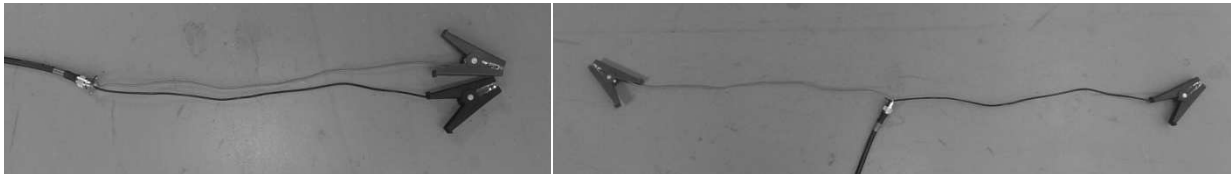


Fig. 2 The extreme position test, The closest position (left) and the furthest position (right) of the clamps. The higher limit of the frequency range is determined by this test.

Results and Analysis

The steps towards the measurement of the scattering parameters of a helium gas cooled superconducting cable are explained in detail in the following practical example (Figure 3). The structure of the connecting device used for the measurement is explained in the section above. The extreme position test for the clamp connectors shows that the movement of the clamps does

not have a significant effect on the measurement in frequencies lower than 20 MHz (Figure 5), which sets the upper limit to 10 MHz. As it is shown in Figure 3 The magnitude of the reflection parameters start to approach the noise level which is higher than the value specified in the instrument manual because of the two pairs of unshielded wires which are prone to environment noise. Therefore, the scattering parameters near the noise level cannot be relied on. In the further simulations, the lower frequency limit was set to 1 kHz and the data set was linearly extrapolated down to the DC point. The lower frequency limit determines the maximum useful value of the IF bandwidth, which is 500 Hz in this case.

Figure 4 shows the impedance between the center conductor and the shield of the cable seen from port 1 obtained from the conversion of the scattering parameters data. Considering that the phase is very close to -90° from 1 kHz up to 200 kHz, it can be concluded that the coupling between the conductor and the shield is highly capacitive in that range and therefore, the aforesaid impedance can be approximated by a single capacitor of 48 nF, calculated at 1 kHz. The impedance of such a capacitor was then calculated at 10 kHz, 50 kHz, 100 kHz, 200 kHz, and 300 kHz. The obtained value has been compared to the actual impedance and the results are shown in Table 1. It shows that the actual impedance between the center conductor and the shield can be approximated by the impedance of a capacitor from 1 kHz (where the capacitor value was calculated) to 200 kHz with acceptable error.

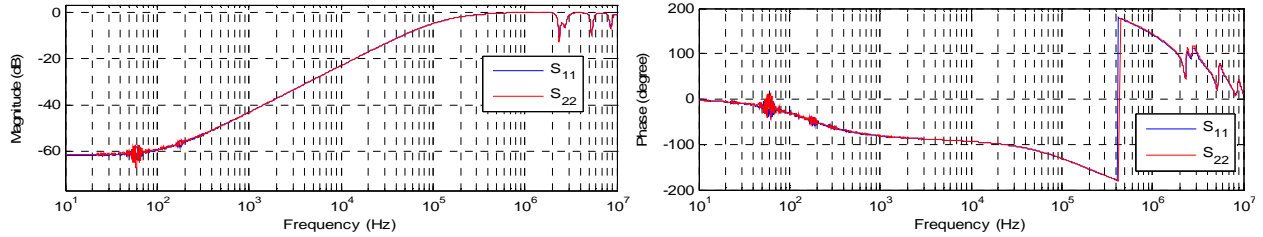


Fig. 3 The reflection scattering parameters (magnitude and phase) of a superconducting cable

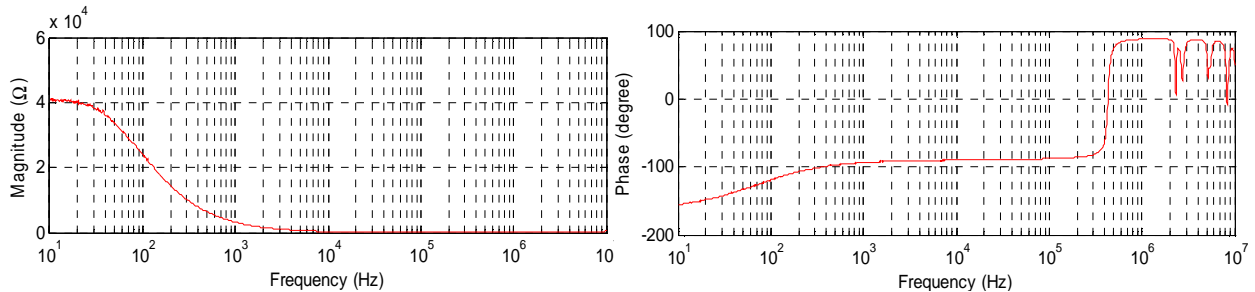


Fig. 4 The impedance magnitude (the left hand side plot) and phase (the right hand side plot) between the center conductor and the shield of the superconducting cable seen from port 1.

Table 1 Comparison of the single capacitor approximation of the ground coupling with the actual impedance value

Frequency point	The capacitor impedance	The actual impedance	Absolute difference %
10 kHz	331.57 Ω	337.9 Ω	1.90
50 kHz	66.31 Ω	66.95 Ω	0.9582
100 kHz	33.157 Ω	32.267 Ω	2.685
200 kHz	16.578 Ω	13.569 Ω	18.153
300 kHz	11.052 Ω	6.047 Ω	45.28

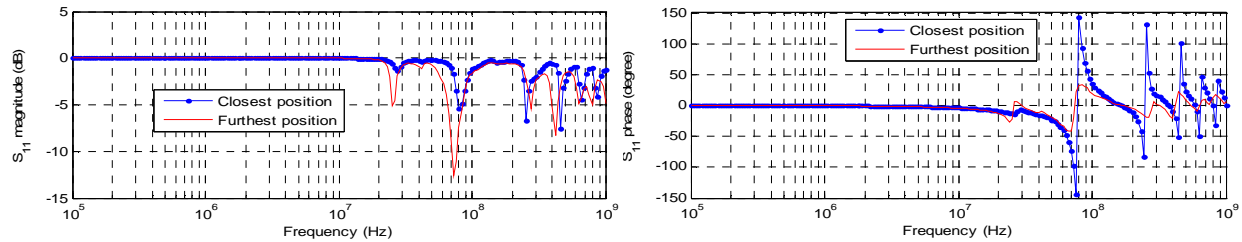


Fig. 5 Fluctuations of the measured data due to the position of the connection clamps with respect to each other in frequencies higher than 10 MHz

Figure 5 illustrates the result of the measurement of S_{11} in extreme position test for the utilized clamps. Evidently, the magnitude and phase of the measured scattering parameters start to deviate when the frequency passes 10 MHz. This justifies using 10 MHz as the upper frequency limit.

Conclusion and Outlook

Trough the paper, the issues in obtaining reliable frequency domain data of high power components, such as the connection leads, setting the frequency limits and IF bandwidth, were addressed. The outcome of the measurement can be used to characterize the coupling of the energized part of the system to ground in a wide frequency range. More accurate models can be built based on reliable measurements, which can help the designers to have a better view of the consequences of different ground faults and therefore optimize the system in an efficient way. The next step would be looking into the application of other microwave engineering analytical tools, such as the mixed mode presentation of the scattering parameters, in modeling the power systems components, such as power cables, and facing the issues and challenges that arise.

References

- [1] B. Jacobson and J. Walker, "Grounding considerations for dc and mixed dc and ac power systems," *Naval Engineers Journal*, vol. 119, no. 2, pp. 49–62, Nov 2007.
- [2] J. Ciezki, L. Graber, S. Pekarek, and M. Steurer, "Evaluation of rail harmonics in alternative MVDC grounding strategies," in *ASNE Electric Machines Technologies Symposium (EMTS)*, Philadelphia, PA, may 2010, pp. 19–20.
- [3] L. Graber, D. Infante, M. Steurer, and W. Brey, "Model validation for shipboard power cables using scattering parameters," *Journal of High Voltage Engineering*, vol. 37, no. 11, 2011.
- [4] L. Graber, M. Steurer, J. Kvitkovic, M. Kofler, S. Pekarek, R. Howard, A. Taher, M. Mazzola, and A. Card, "Time and frequency domain methods to evaluate grounding strategies for medium voltage dc shipboard power systems," in *Electric Ship Technologies Symposium (ESTS), 2013 IEEE*, April 2013, pp. 43–48.
- [5] B. Mohebali, P. Breslend, L. Graber, and M. Steurer, "Validation of a scattering parameter based model of a power cable for shipboard grounding studies," in *ASNE Electric Machines Symposium (EMTS)*, May 2014, pp. 28–29.
- [6] P. Breslend B. Mohebali, L. Graber, M. Steurer, "Simulation of a simplified high frequency equivalent lumped parameter model," Submitted to *ASNE Naval Engineers Journal (NEJ)*, Dec. 2014.

APPENDIX E

High Frequency Models for Rotating Machines in Ungrounded Shipboard Power Systems

Introduction

The all-electric shipboard power system (SPS) has been an ongoing research topic for Electric Ship Research Development Consortium (ESRDC), a division of the Office of Naval Research (ONR) [1]. The proposed integrated power system (IPS) will need detailed models of all electrical components as well as the environment in which the system will operate. The classical methods of system modeling cannot be assumed to directly apply to SPS, considering the physical differences between terrestrial and shipboard applications [2]. The power electronics, cabling, and machines is expected to be subject to electromagnetic interference (EMI) and therefore electromagnetic compatibility (EMC) will need to be explored further [3], [4]. Models which capture the electromagnetic interaction between the SPS and ship hull ground (SHG) are important for grounding considerations such as fault location algorithms based on noise pattern analysis [5], [6]. The IPS models will also mitigate issues prior to building the ship and reduce equipment sizing through optimization and proper placement of components to lower HF content in the system.

The IPS preferred configuration will be a DC distribution network for many reasons including the ability to operate under certain fault conditions and it does not hold the same issues found in AC distribution [7]. The rectification and inversion of current by switched mode converters is known to produce EMI due to the increase in dv/dt and switching frequencies [8]. Substantial research has been covered in describing transient behavior and its undesired HF effects on power systems [9]-[15].

The EMI in the system will need to be accurately characterized with wideband frequency models to properly study the effects of different grounding strategies. Models must be able to also represent the parasitic coupling effects of SPS and the SHG. The parasitic coupling provides a low impedance path back to the source of the HF transients resulting in common-mode (CM) and differential-mode (DM) currents [16]-[18].

High frequency (HF) transient models have been developed for cables, power electronic devices, and machines in [19], [20], and [21] respectively. The common methods or techniques used to develop the current HF models can be highly complex and specialized to each type of device in order to capture the entire band of frequencies [8]. Techniques used to extract model parameters of various components have been developed primarily through analytical assumptions, lumped parameters, and finite element analysis [22].

Simulation of a simplified high frequency equivalent lumped parameter model

Models that characterize a wide frequency spectrum have been proposed in literature to predict all types of transients and EMI behavior to limit the stress leading to insulation and bearing failures [23]. A base line for HF models needs to be established in order to compare other models on their accuracy, ease of calculation, and flexibility of implementation for multiple grounding scenarios. The base model is developed using a conventional method of lumped parameter equivalent circuits

(ECs) with parameter values extracted from impedance measurements. The equivalent T-circuit has three phase terminals consisting of two resistive-inductive (RL) components split by a capacitance (C) to ground on each phase and a wye connected neutral.

An unloaded generator spinning at rated speed will produce alternating phase voltages that are a function of the rotor revolutions and the number of pole pairs. When a terminal is shorted to ground the reflected voltage is reflected back into the machine and contains a wide spectrum of frequencies corresponding to the inverse of the fall time. The parasitic capacitances of the machine will provide a low impedance path to ground at higher frequencies, closing the ground path, creating a transient current in the ground back to the source of the fault [19], [24].

To simulate the fault scenario the capacitors and inductors are given initial voltage and current values corresponding to the phase voltages and currents of an unloaded system at steady state. The simulation consists of an unloaded permanent magnet synchronous machine (PMSM) model with the neutral point ungrounded and terminal T1 faulting to ground (Fig. 1).

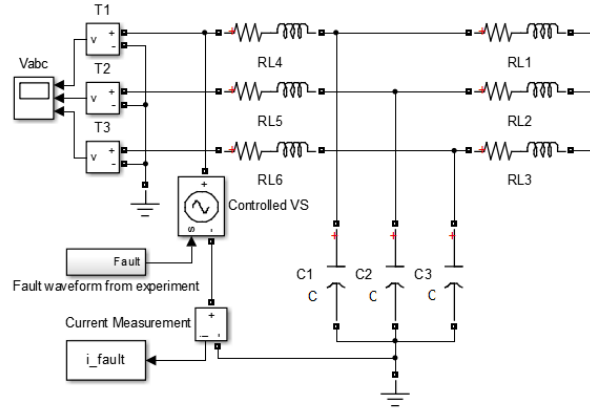


Fig. 1. PMSM HF fault simulation using experimental measured fault to trigger a controlled voltage source coupling terminal T1 to ground with terminals T2 and T3 unloaded.

The short circuit voltage to ground is characterized to match the experimental fault waveform by using a controlled voltage source and providing the experimentally measured waveform. The simulated fault current can be seen in Fig. 2.

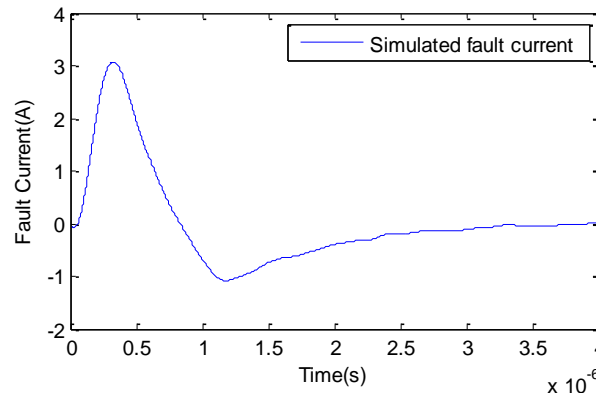


Fig. 2. Simulated fault current using a simplified HF lumped parameter model.

The model values were parameterized based on impedance measurements of the PMSM available for measurement testing [25]. An impedance analyzer (IA) was used to measure the AC machine impedance response from 100 Hz to 10 MHz and plotted with the frequency response of the lumped model seen in Fig. 3.

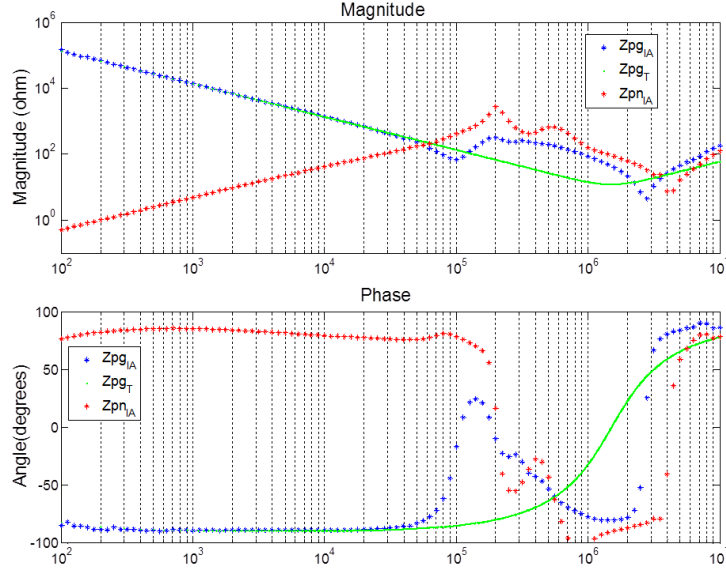


Fig. 3. PMSM measured phase to ground impedance Z_{pgIA} and modeled phase to ground impedance Z_{pgT} are plotted as a function of frequency and used to calculate capacitances. The phase to neutral impedance Z_{pnIA} is also plotted and used to calculate RL parameter values.

PMSM fault response experiment to capture high frequency transient current

An unloaded 8 pole 17 kW PMSM rotating at nominal speed is setup for a terminal fault to ground via solid state relay (SSR). The terminal voltages are measured with a differential probe that has CM rejection capability to ensure an isolated measurement. Terminal T1 voltage is relayed through to control logic that determines the next positive edge zero crossing, calculates a 90° phase shift, and sets the terminal fault signal initiation at the peak voltage. The controls then outputs an analog 10 V_{DC} signal to activate the SSR and trigger an oscilloscope to capture the HF transient response. The results can be seen in Fig. 4 where the top plot displays fault current and the bottom plot displays terminal voltages T1, T2, and T3.

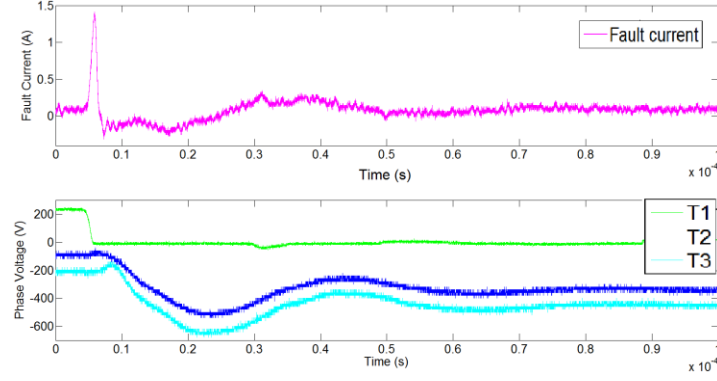


Fig. 4. Measured fault current and corresponding HF terminal voltage responses of a PMSM.

Proposed S-parameter approach advantages and considerations

The proposed Scattering parameter approach for modeling has been defined in the companion papers [26], [27] explaining how measurements are to be conducted on SPS components. The network parameters defining reflection and transmission coefficients for measured frequency vectors of n-port devices are defined in [28]. The measurement setup for the PMSM machine seen in Fig. 5 details the voltage waveforms measured at each port of the 4-port network.

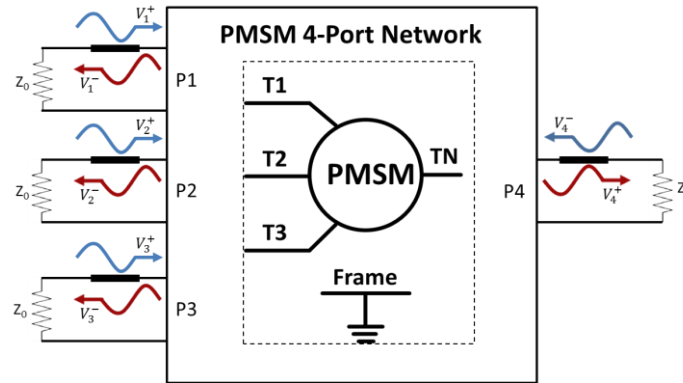


Fig. 5. Voltages waveforms corresponding to the 4-port PMSM network with $Z_0 = 50 \Omega$ both VNA cables and both single ended terminations.

Two network ports are measured by the ports of the vector network analyzer (VNA) while the other two ports are terminated with a 50Ω single ended termination and defined in [26].

To verify scattering measurements of AC machines first we needed to compare rotor positions and the affect it has on the stator measurements. In [8] it was concluded that impedance response measurements had substantial error due to rotor position affects below the first resonance frequency. Three rotor positions were chosen 0° , 270° , and 345° corresponding to three different cogging positions. S-parameters were measured at each position on a 250 W PMSM and the resulting maximum deviation in rotor position had only 0.4 dB difference in the lower frequency ranges. Measurements were also carried out on an asynchronous machine and the deviations were also found to be insignificant with a maximum value less than 0.025 dB.

The 4-port scattering model can also be measured to mimic conventional experimental impedance measurement techniques typically used for extraction of parametric values used to determine ECs for AC machines. The scattering measurements of 3 different 1-port configurations were converted into phase-to-neutral, common-mode, and differential-mode impedances and verified with a 2.5 MW squirrel cage induction (SCI) machine and a 17 kW PMSM seen in figure (6a) and figure (6b) respectively.

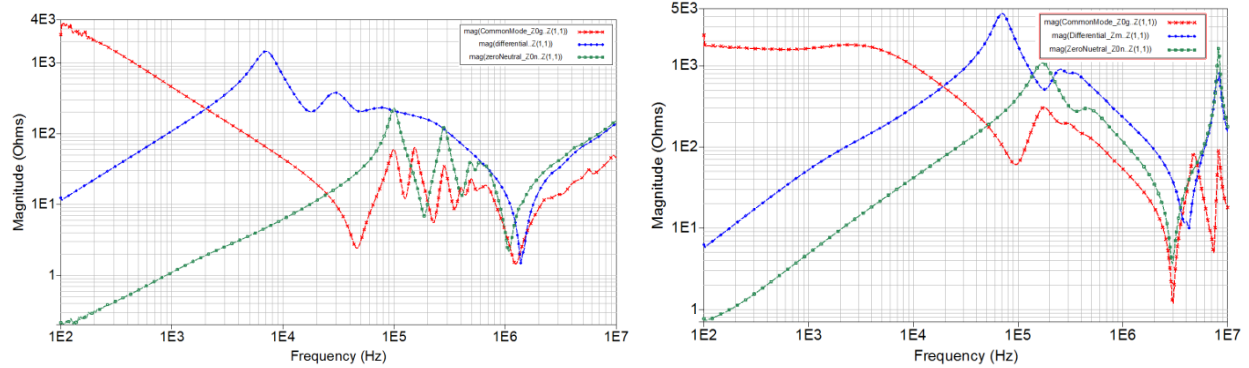


Fig. 6. Impedance magnitudes for phase-to-neutral, common-mode, and differential-mode versus frequency for a (a) 2.5 MW SCI and (b) 17 kW PMSM.

The impedance plots in Fig. 6 capture more resonances and anti-resonances than found using any equivalent circuit, finite element analysis (FEA), frequency response function (FRF), or stand still frequency response (SSFR) techniques given in previous literature [25], [29]-[31]. This is a substantial step in the direction to develop accurate models for the future all-electric IPS.

Conclusions and future considerations

The fault current in an experiment with a PMSM was not accurately captured by the lumped EC model. This conventional method is not recommended for fast transients as they occur during faults. It has been determined that measuring S-parameters over a wide frequency range and integrating them in a power system simulation is a valid process to measure HF power components and can be used to develop more accurate and reliable measurement models for grounding studies. The proposed method of using S-parameters as HF models of machines has not been attempted. Further research is needed to thoroughly investigate the way it will be implemented in various modeling platforms like Agilent Design Systems, MATLAB/Simulink, etc.

Future work will use S-parameters to simplify the development of HF generator and motor models. The bearing contact impedances between stator and rotor are difficult to model due to the bearing contact impedance when motor is at standstill [32]. The incorporation of aging and winding pollution effects due to the environment to predict failures or schedule maintenance could also be determined [33], [34]. Future work will need to determine the impact of these effects and the errors associated with measuring [35] to produce updated scattering matrices for more accurate results.

References

- [1] N. Schulz, R. Hebner, S. Dale, R. Dougal, S. Sudhoff, E. Zivi, and C. Chrysostomidis, "The U.S. ESRDC advances power system research for shipboard systems," in Universities Power Engineering Conference, 2008. UPEC 2008. 43rd International, Sept 2008, pp. 1–4.
- [2] L. Graber, M. Steurer, J. Kvitkovic, M. Kofler, S. Pekarek, R. Howard, A. Taher, M. Mazzola, and A. Card, "Time and frequency domain methods to evaluate grounding strategies for medium voltage dc shipboard power systems," in Electric Ship Technologies Symposium (ESTS), IEEE, April 2013, pp. 43–48.
- [3] L. Arnedo and K. Venkatesan, "High frequency modeling of induction motor drives for EMI and overvoltage mitigation studies," in Electric Machines and Drives Conference, 2003. IEMDC'03. IEEE International, vol. 1, June 2003, pp. 468–474 vol.1.
- [4] Y. Pan, M. Steurer, and T. Baldwin, "Ground fault location testing of a noise-pattern-based approach on an ungrounded dc system," Industry Applications, IEEE Transactions on, vol. 47, no. 2, pp. 996–1002, March 2011.
- [5] Y. Pan, M. Steurer, and T. Baldwin, "Feasibility study of noise pattern analysis based ground fault locating method for ungrounded dc shipboard power distribution systems," in Electric Ship Technologies Symposium (ESTS), 2009. IEEE, April 2009, pp. 18–22.
- [6] H. Hamilton and N. Schulz, "Impact of grounding on overcurrents for a naval ac/dc shipboard power system," in Power Symposium, 2007. NAPS '07. 39th North American, Sept 2007, pp. 170–176.
- [7] B. Mirafzal, G. Skibinski, R. Tallam, D. Schlegel, and R. Lukaszewski, "Universal induction motor model with low-to-high frequency-response characteristics," Industry Applications, IEEE Transactions on, vol. 43, no. 5, pp. 1233–1246, Sept 2007.
- [8] E. Zhong, T. Lipo, and S. Rossiter, "Transient modeling and analysis of motor terminal voltage on pwm inverter-fed ac motor drives," in Industry Applications Conference, 1998. Thirty-Third IAS Annual Meeting. The 1998 IEEE, vol. 1, Oct 1998, pp. 773–780 vol.1.
- [9] R. Kerkman, D. Leggate, and G. Skibinski, "Interaction of drive modulation and cable parameters on ac motor transients," Industry Applications, IEEE Transactions on, vol. 33, no. 3, pp. 722–731, May 1997.
- [10] I. Metwally, "Simulation of the impulse response of electrical machines," Energy Conversion, IEEE Transactions on, vol. 14, no. 4, pp. 861–867, Dec 1999.
- [11] E. Persson, "Transient effects in application of pwm inverters to induction motors," Industry Applications, IEEE Transactions on, vol. 28, no. 5, pp. 1095–1101, Sep 1992.
- [12] A. Bonnett, "Analysis of the impact of pulse-width modulated inverter voltage waveforms on ac induction motors," Industry Applications, IEEE Transactions on, vol. 32, no. 2, pp. 386–392, Mar 1996.
- [13] J. Guardado, V. Carrillo, and K. Cornick, "Calculation of interturn voltages in machine windings during switching transients measured on terminals," Energy Conversion, IEEE Transactions on, vol. 10, no. 1, pp. 87–94, Mar 1995.
- [14] C. Petrarca, G. Lupo, L. Egiziano, V. Tucci, and M. Vitelli, "Steepfronted overvoltages in inverter-fed induction motors: numerical identification of critical parameters," in High Voltage Engineering, 1999. Eleventh International Symposium on (Conf. Publ. No. 467), vol. 5, 1999, pp. 433–436 vol.5.

- [15] G. Grandi, D. Casadei, and U. Reggiani, "Analysis of common- and differential-mode hf current components in pwm inverter-fed ac motors," in Power Electronics Specialists Conference, 1998. PESC 98 Record. 29th Annual IEEE, vol. 2, May 1998, pp. 1146–1151 vol.2.
- [16] G. Grandi, D. Casadei, and U. Reggiani, "Common- and differential-mode hf current components in ac motors supplied by voltage source inverters," Power Electronics, IEEE Transactions on, vol. 19, no. 1, pp. 16–24, Jan 2004.
- [17] W. Shen, F. Wang, D. Boroyevich, and Y. Liu, "Definition and acquisition of cm and dm emi noise for general-purpose adjustable speed motor drives," in Power Electronics Specialists Conference, 2004. PESC 04. 2004 IEEE 35th Annual, vol. 2, June 2004, pp. 1028–1033 Vol.2.
- [18] H. De Paula, D. de Andrade, M. Chaves, J. Domingos, and M. de Freitas, "Methodology for cable modeling and simulation for high-frequency phenomena studies in pwm motor drives," Power Electronics, IEEE Transactions on, vol. 23, no. 2, pp. 744–752, March 2008.
- [19] W. Shen, F. Wang, and D. Boroyevich, "Conducted emi characteristic and its implications to filter design in 3-phase diode front-end converters," in Industry Applications Conference, 2004. 39th IAS Annual Meeting. Conference Record of the 2004 IEEE, vol. 3, Oct 2004, pp. 1840–1846.
- [20] A. Moreira, T. Lipo, G. Venkataramanan, and S. Bernet, "High frequency modeling for cable and induction motor overvoltage studies in long cable drives," in Industry Applications Conference, 2001. Thirty-Sixth IAS Annual Meeting. Conference Record of the 2001 IEEE, vol. 3, Sept 2001, pp. 1787–1794 vol.3.
- [21] B. Revol, J. Roudet, J.-L. Schanen, and P. Loizelet, "Emi study of three-phase inverter-fed motor drives," Industry Applications, IEEE Transactions on, vol. 47, no. 1, pp. 223–231, Jan 2011.
- [22] S. Ogasawara, H. Ayano, and H. Akagi, "Measurement and reduction of emi radiated by a pwm inverter-fed ac motor drive system," Industry Applications, IEEE Transactions on, vol. 33, no. 4, pp. 1019–1026, Jul 1997.
- [23] R. Schiferl, M. Melfi, and J. Wang, "Inverter driven induction motor bearing current solutions," in Petroleum and Chemical Industry Conference, 2002. Industry Applications Society 49th Annual, 2002, pp. 67–75.
- [24] L. Wang, C.-m. Ho, F. Canales, and J. Jatskevich, "High-frequency cable and motor modeling of long-cable-fed induction motor drive systems," in Energy Conversion Congress and Exposition (ECCE), 2010 IEEE, Sept 2010, pp. 846–852.
- [25] B. Mohebbi, P. Breslend, L. Graber, and M. Steurer, "Validation of a scattering parameter based model of a power cable for shipboard grounding studies," in ASNE Electric Machines Symposium (EMTS), May 2014, pp. 28–29.
- [26] B. Mohebbi, P. Breslend, L. Graber, and M. Steurer, "How to measure scattering parameters for modeling components of shipboard power systems," Submitted in ASNE Naval Engineers Journal (NEJ), Dec. 2014.
- [27] J. Wei, D. Gerling, and M. Galek, "S-parameters characterization and sequence model of three-phase emi filter," in Industrial Electronics Society, IECON 2013 - 39th Annual Conference of the IEEE, Nov 2013, pp. 1254–1259.
- [28] R. Escarela-Perez, T. Niewierowicz, and E. Campero-Littlewood, "Synchronous machine parameters from frequency-response finite-element simulations and genetic algorithms," Energy Conversion, IEEE Transactions on, vol. 16, no. 2, pp. 198–203, Jun 2001.
- [29] A. Repo and A. Arkkio, "Numerical impulse response test to estimate circuit-model parameters for induction machines," Electric Power Applications, IEE Proceedings -, vol. 153, no. 6, pp. 883–890, November 2006.

- [30] A. Keyhani and H. Tsai, "Identification of high-order synchronous generator models from ssfr test data," *Energy Conversion, IEEE Transactions on*, vol. 9, no. 3, pp. 593–603, Sep 1994.
- [31] A. Muetze and A. Binder, "Calculation of motor capacitances for prediction of the voltage across the bearings in machines of inverter based drive systems," *Industry Applications, IEEE Transactions on*, vol. 43, no. 3, pp. 665–672, May 2007.
- [32] W. Liu, E. Schaeffer, D. Averty, and L. Laron, "A new approach for electrical machine winding insulation monitoring by means of high frequency parametric modeling," in *IEEE Industrial Electronics, IECON 2006 - 32nd Annual Conference on*, Nov 2006, pp. 5046–5050.
- [33] W. Liu, E. Schaeffer, D. Averty, and L. Laron, "A new approach for form wound machine goundwall insulation diagnosis by means of high frequency model parameter monitoring," in *Industrial Electronics, 2007. IEEE International Symposium on*, June 2007, pp. 1270–1275.
- [34] I. Rolfes and B. Schiek, "Multiport method for the measurement of the scattering parameters of n-ports," *Microwave Theory and Techniques, IEEE Transactions on*, vol. 53, no. 6, pp. 1990–1996, June 2005.

APPENDIX F

Modeling of Common-mode Currents on Electric Ship Architectures

Mississippi State University
Department of Electrical and Computer
Engineering

Michael Mazzola and Maryam Rahmani

Presented by Michael Mazzola

This work was supported by the Office of Naval Research as part of the Electric Ship Research and Development Consortium under Grant N00014-08-1-0080.



MISSISSIPPI STATE
UNIVERSITY™



Grounding Team



Lukas Graber (lead)
Mischa Steurer
Jozef Kvitkovic

Student:
Patrick Breslend



Steve Pekarek

Students:
Aaron Brovont



MISSISSIPPI STATE
UNIVERSITY

Michael Mazzola
Angela Card

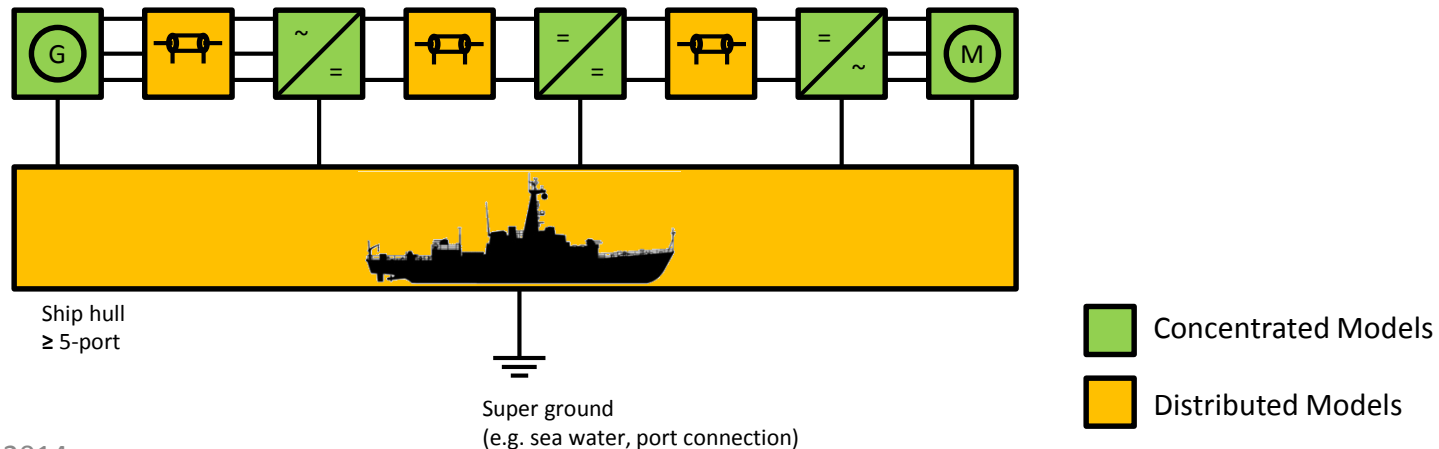
Student:
Maryam Rahmani

External Collaboration:
W. Blake, B. Hood, K. Watts



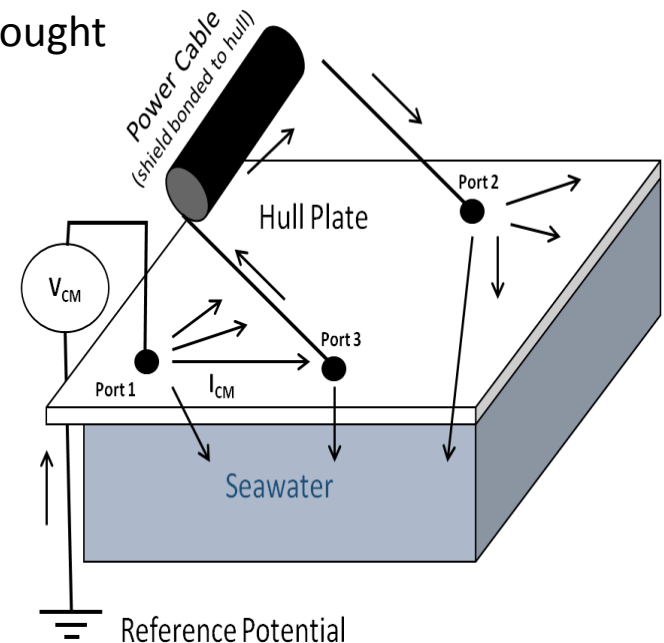
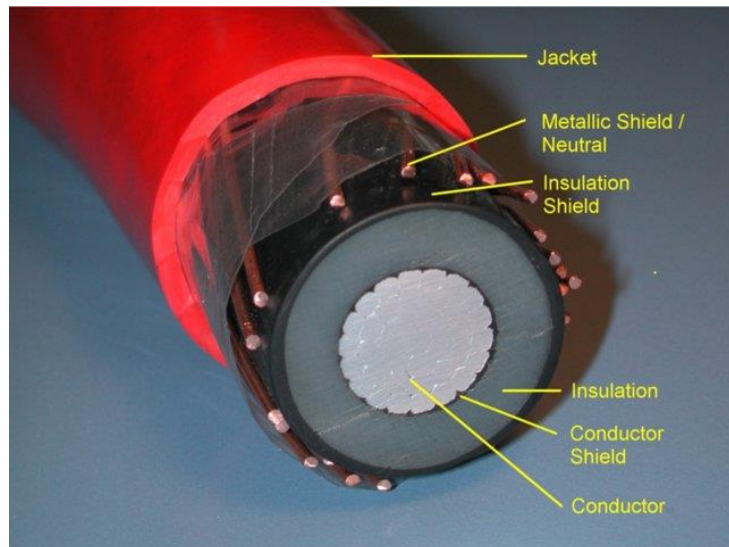
Concentrated and Distributed Models

- Grounding models for power cables
 - Lumped element models (pi-sections)
 - Distributed models (PSCAD: freq. dep. phase model)
 - S-parameter models (ADS, MATLAB, Empirical)
- Grounding models for power electronics
 - DC-DC converter (S-parameter; MATLAB)
 - Inverter (not completed)
- Grounding models for rotating machines
 - Lumped element models (T-model; SimPowerSystems, PLECS)
 - S-parameter models (ADS)
- Ship hull (ADS)

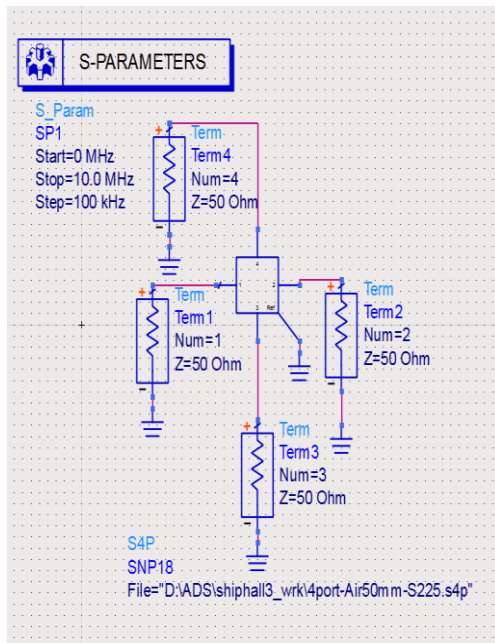
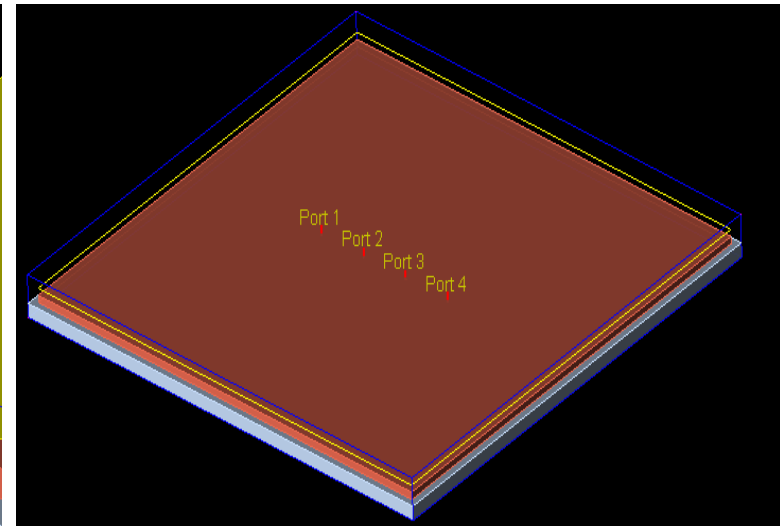
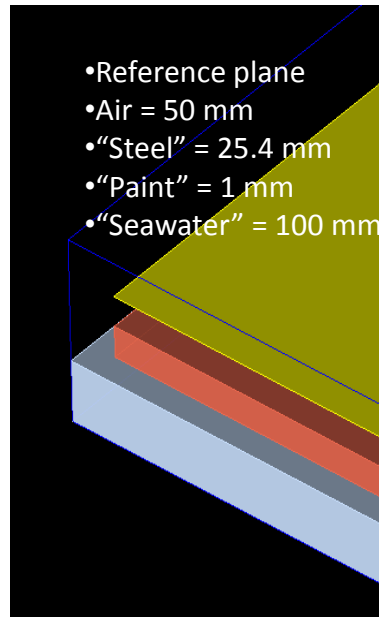
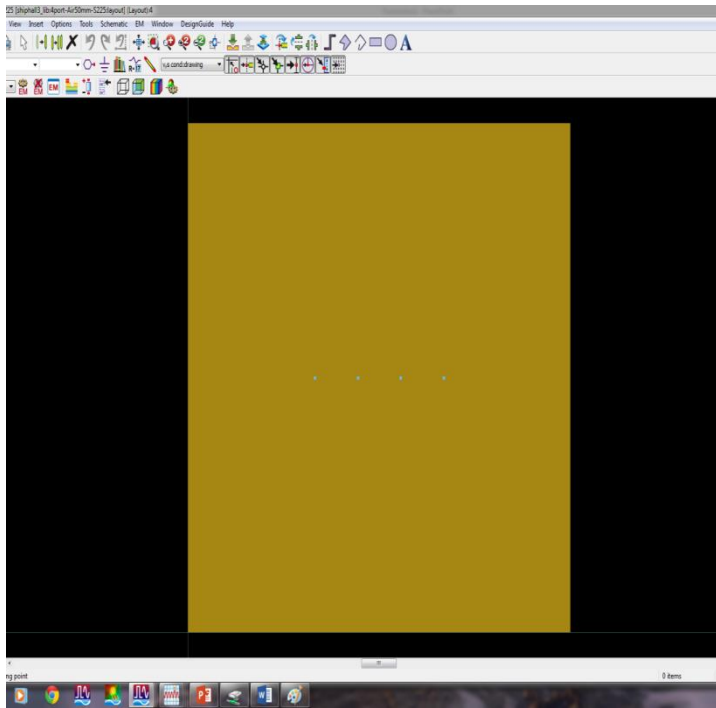


Common-Mode Current on the Hull and Bulkheads

- Demonstrate behavioral modeling tools for hull and interconnected grounded conductors derived from physics based simulation.
 - Many grounded conductors bonded to hull and forming interconnected network on which common-mode current is impressed (e.g., cable sheaths)
 - Model with multi-port system based on, or derived from, S-parameters
 - ADS computes S-parameters for hull & bulkhead geometries with N bonds
 - Network analyzer measures three-terminal S-parameters for cables
 - Synchronizing reference potential requires careful thought

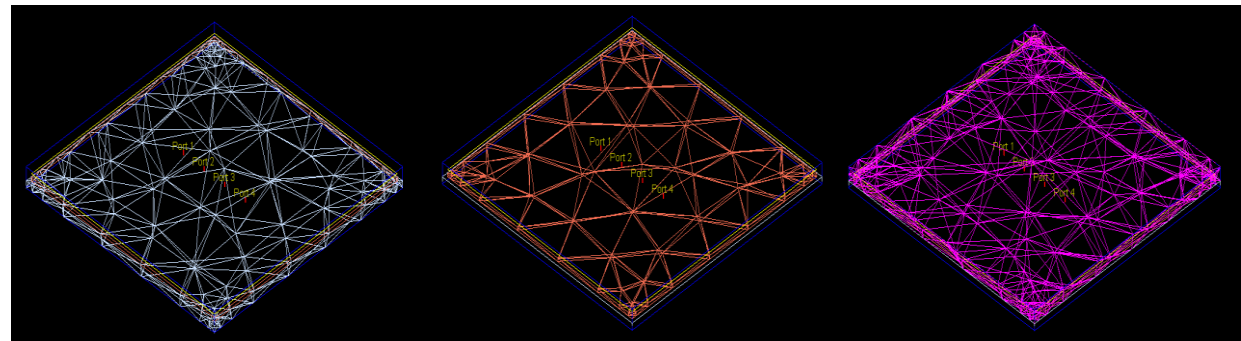


S-Parameters of Open-Form Conductor Systems



Physics based calculation of S-parameter model of a four-port square block in Agilent ADS

- Finite element analysis with auto-generated mesh
- Frequency range is zero to 10 MHz



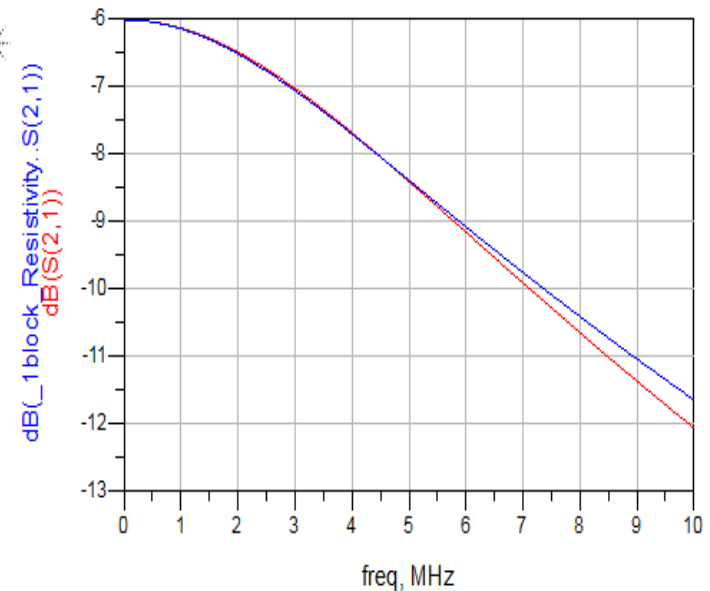
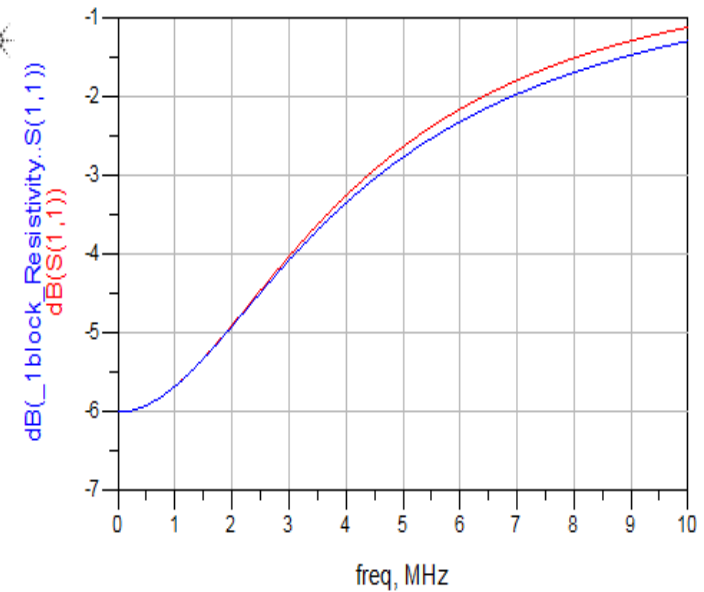
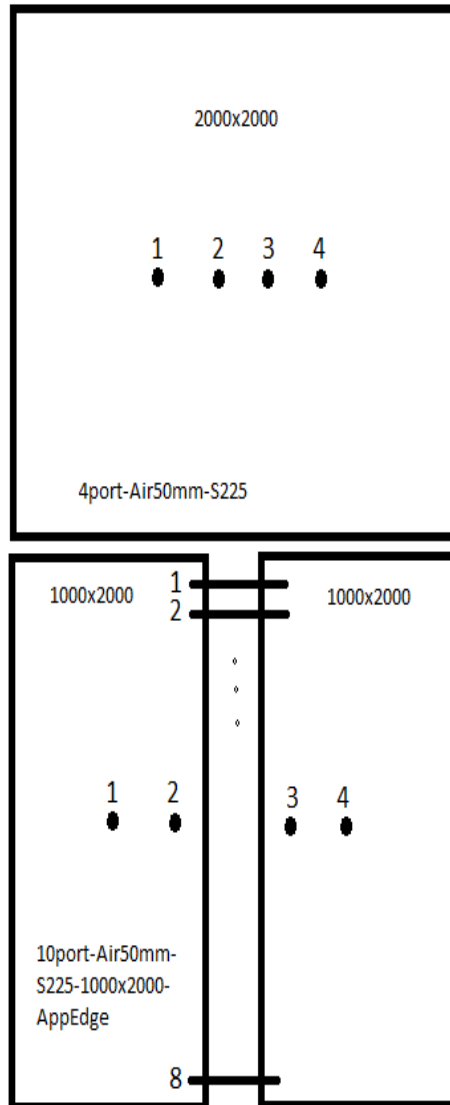


Physics based calculation of S-parameter model of elementary rectangle in ADS

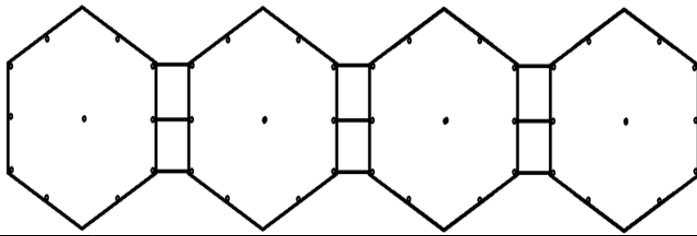
- Finite element analysis with auto-generated mesh
- Edge ports to interconnect elementary rectangles to form a single square
- Frequency range is zero to 10 MHz



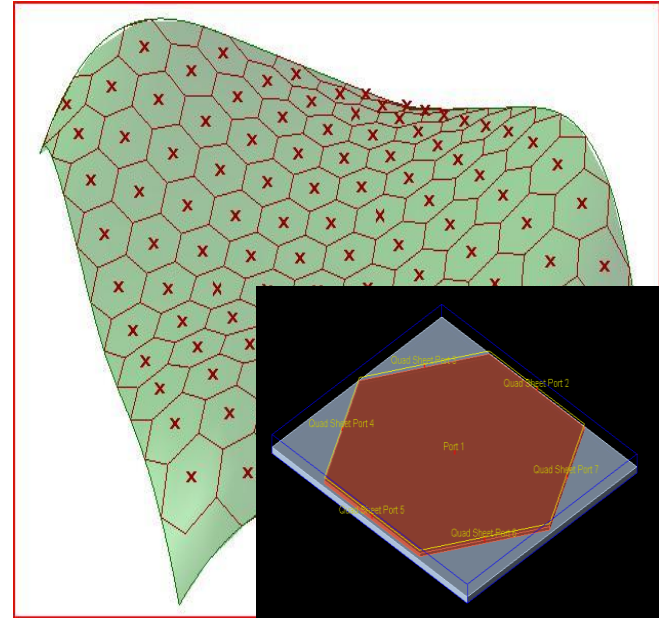
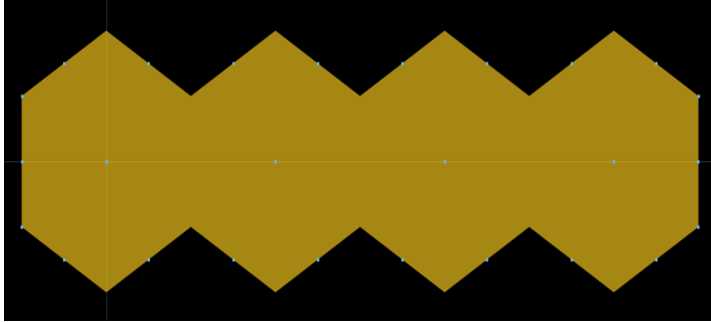
Comparison of equivalent S-parameters in ADS formed from a single block and a composite block made of two elementary rectangles



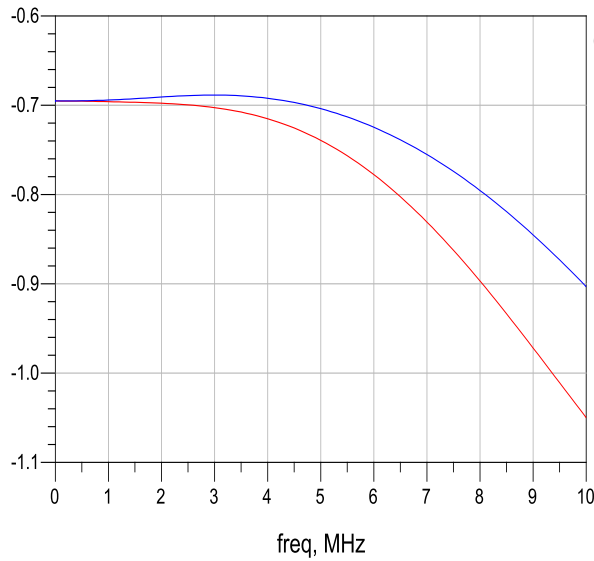
Discrete



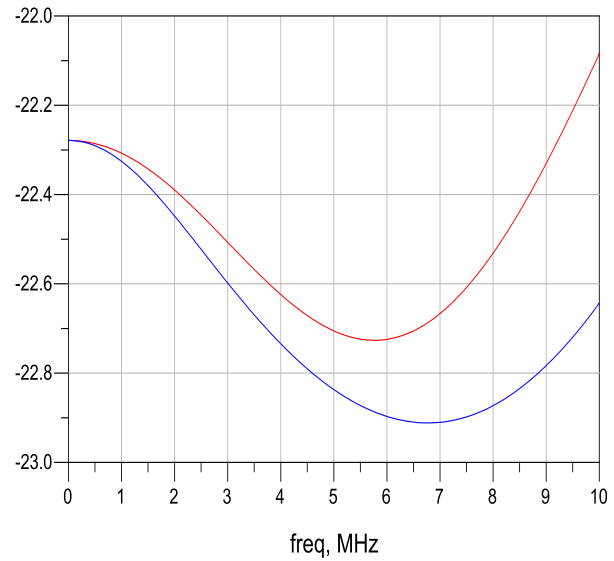
Continuous

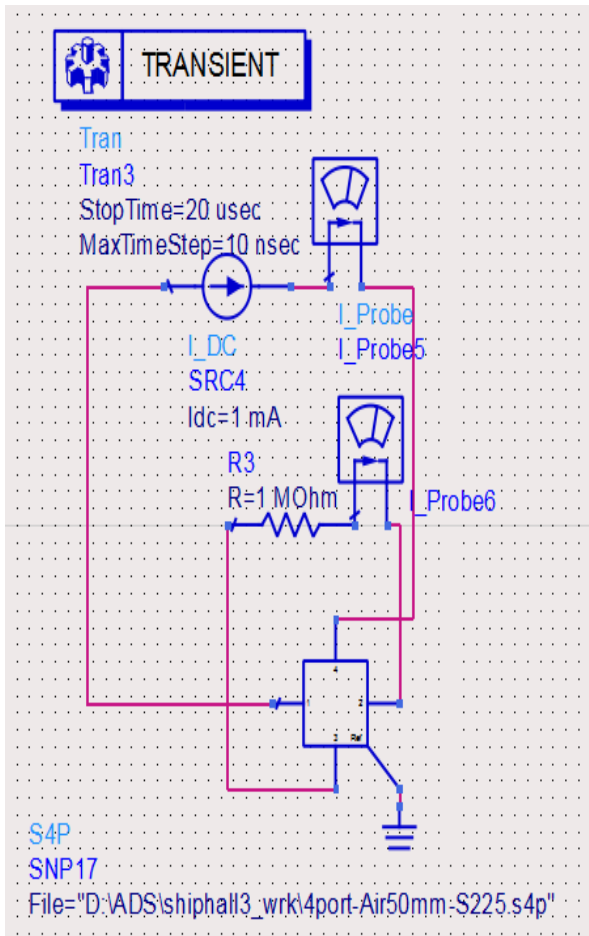


dB(_11port_Air50mm_Hexagon_AppEdge_4_cacaded_FEM..S(1,1))
dB(S(1,1))

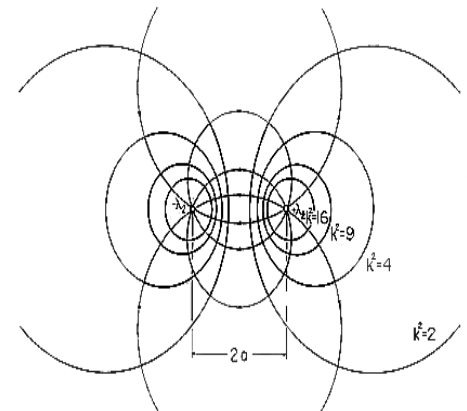
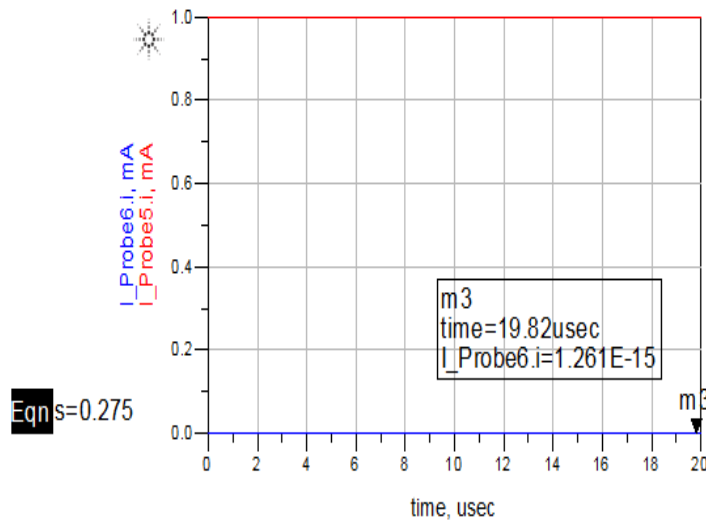


dB(_11port_Air50mm_Hexagon_AppEdge_4_cacaded_FEM..S(2,1))
dB(S(2,1))





Verification of numerical four-port model with solution to parallel line-charge electrostatic solution



$$\text{Eqn } x=1.5*s \quad \text{Eqn } a=s/2 \quad \text{Eqn } w=0.0254 \quad \text{Eqn } \text{Phi}=0.5*1e6*m3 \quad \text{Eqn } l=1e-3$$

$$\text{Eqn } \text{Sigma1}=l/(2*pi*Phi*w)*\ln((x+a)/(x-a)) \quad \text{Eqn } \text{Sigma2}=l/(2*pi*Phi*w)*\ln(-(x+a)/(x-a))$$

time	Sigma2	Sigma1	Phi	a	w	x	m2 <invalid>
19.82 usec	3.198E7 / 77.558	6.891E6	6.303E-10	0.138	0.025	0.413	

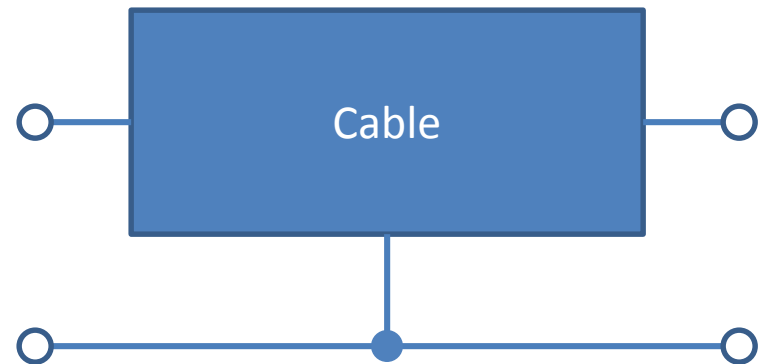
S-Parameters of Cables

Empirically Derived

Network Analyzer connected to cable ends through removable coaxial terminations



Are the ports the center conductor or the shield?

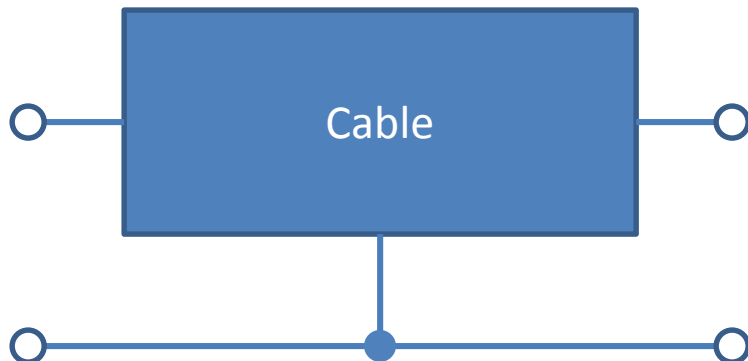


- For power system the ports are the center conductor.
- For the safety grounding system the ports are the sheaths.

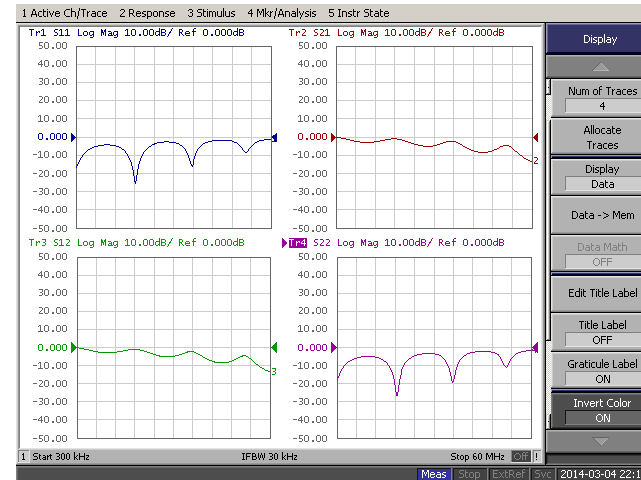
S-Parameters of Cables

Empirically Derived

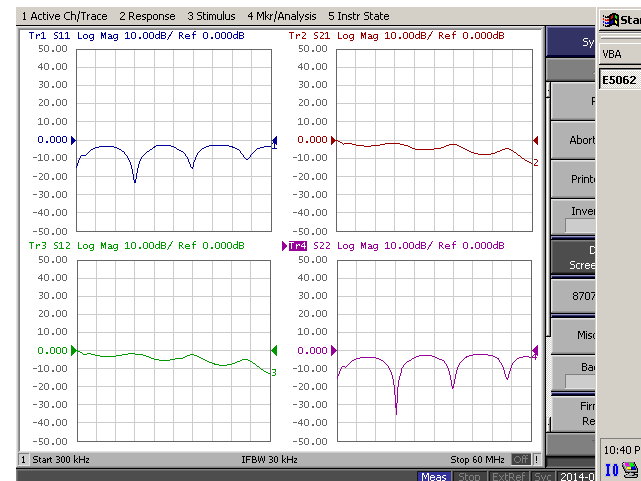
S-parameter model is symmetrical



- Measure at center conductor.
- Reference third terminal at:
 - Hull potential in power system simulation
 - Power bus potential in hull system simulation.



center
conductor



shield
conductor

Summary

- Ship power systems are evolving in complexity to the point where design automation is essential.
- Simulation and modeling of a large open-form conductor system (ship) using finite element analysis too cumbersome for early stage design.
- Problem can be solved by converting to behavioral models derived from physics-based modeling supplemented with empirical data.
- “Arbitrary” open-form conductor systems built up from elementary behavioral models.

